MOUNTAIN-PLAINS CONSORTIUM

IMPACT OF MOBILITY AS A SERVICE ON TRANSIT ACCESS

Technical Report Documentation Page

1. Report No. MPC-608	2. Government Accession No.	3. Recipient's Catalog No.	
4. Title and Subtitle Impact of Mobility as a Service on Transit Access		5. Report Date March 2022	
		6. Performing Organization Code	
7. Author(s) X.C. Liu Y. Zhou N. Haghighi		8. Performing Organization Report No. MPC 22-453	
9. Performing Organization Name and Address University of Utah 110 Central Campus Drive, Suite 2000 Salt Lake City, UT 84112		10. Work Unit No. (TRAIS)	
		11. Contract or Grant No.	
12. Sponsoring Agency Name and Address Mountain-Plains Consortium North Dakota State University PO Box 6050, Fargo, ND 58108		13. Type of Report and Period Covered Final Report	
		14. Sponsoring Agency Code	
15. Supplementary Notes Supported by a grant from the US DOT, University Transportation Centers Program			

16. Abstract

The emergence of a new mode, Mobility as a Service (MaaS), has, to date, been most often characterized as the ridehailing mode provided by companies such as Uber and Lyft. This study focuses on MaaS as a transit access mode. This mode is also referred to as microtransit. For this research, we describe the technical modeling steps required to account for this new transit access mode. Using Wasatch Front Travel Demand Model as a case study, this project details the steps involved so that this work can be carried forward. Further, using the microtransit pilot project launched in Salt Lake City, Utah, we applied big data techniques to model the spatio-temporal pattern of microtransit activities. This work is significant as the research period has undergone the impact of COVID-19, and it represents the first of its kind to offer insights into how COVID-19 altered travel behavior. Specifically, eigendecomposition delineated the homogeneity and heterogeneity of travel patterns across temporal dimensions. We identified first mile/last mile trips as a major source of variance in both pre- and post-COVID periods and that transit-dependent users prove to be inelastic despite the threat of COVID-19. The k-clique percolation method detected possible community formations and tracked how these communities evolved during the pandemic. In addition, we systematically analyzed overlapping communities and the network structure around shared nodes by using a clustering coefficient. The framework can also help transit agencies with performance evaluation, regional transport strategies, and optimal vehicle dispatching.

17. Key Word access, autonomous vehicles, connected vehicles, demand responsive transportation, impacts, mobility, modal split, public transit, ridership, vehicle miles of travel		18. Distribution Statement Public distribution	

19. Security Classif. (of this report)
    Unclassified
	20. Security Classif. (of this page)
	    Unclassified
		21. No. of Pages
		    41
			22. Price
			    n/a

Form DOT F 1700.7 (8-72)   Reproduction of completed page authorized

IMPACT OF MOBILITY AS A SERVICE ON TRANSIT ACCESS

Xiaoyue Cathy Liu, Ph.D., P.E.
Associate Professor
Department of Civil and Environmental Engineering
University of Utah
Salt Lake City, Utah, 84112
Phone: (801) 587-8858
Email: cathy.liu@utah.edu

Yirong Zhou
Ph.D. Student
Department of Civil & Environmental Engineering
University of Utah
110 Central Campus Dr. RM 1650
Salt Lake City, Utah, 84112
Email: Yirong.Zhou@utah.edu

Nima Haghighi, Ph.D.
Transportation Planner II
Planning and Development Department
Pasco County
8731 Citizens Drive, Suite 360
New Port Richey, FL 34654
Phone: (727) 847-8142
Email: nhaghighi@pascocountyfl.net

March 2022

Acknowledgements

The authors acknowledge the Mountain-Plain Consortium (MPC) and the Utah Department of Transportation (UDOT) for funding this research, and the following individuals from UDOT serving on the Technical Advisory Committee (TAC) for helping to guide the research:

- Richard Brockmyer (UDOT)
- Khaisy Vonarath (UDOT)

The authors would also like to acknowledge Bert Granberg and Chad Worthen of WFRC, Tim Hereth of MAG, and Shana Lindsay from UDOT Research who served as project manager.

Disclaimer

The contents of this report reflect the views of the authors, who are responsible for the facts and the accuracy of the information presented. This document is disseminated under the sponsorship of the Department of Transportation, University Transportation Centers Program, in the interest of information exchange. The U.S. Government assumes no liability for the contents or use thereof.

ABSTRACT

The emergence of a new mode, mobility as a service (MaaS), has, to date, been most often characterized as the ride-hailing mode provided by companies such as Uber and Lyft. This study focuses on MaaS as a transit access mode. This mode is also referred to as microtransit. For this research, we describe the technical modeling steps required to account for this new transit access mode. Using Wasatch Front Travel Demand Model as a case study, this project details the steps involved so this work can be carried forward. Further, using the microtransit pilot project launched in Salt Lake City, Utah, we applied big data techniques to model the spatio-temporal pattern of microtransit activities. This work is significant as the research period has undergone the impact of COVID-19, and it represents the first of its kind to offer insights into how COVID-19 altered travel behaviors. Specifically, eigendecomposition delineated the homogeneity and heterogeneity of travel patterns across temporal dimensions. We identified first-mile/last-mile trips as a major source of variance in both pre- and post-COVID periods and that transit-dependent users prove to be inelastic despite the threat of COVID-19. The k-clique percolation method detected possible community formations and tracked how these communities evolved during the pandemic. In addition, we systematically analyzed overlapping communities and the network structure around shared nodes by using a clustering coefficient. The workflow developed in this research broadly is generalizable and valuable for understanding the unique spatio-temporal patterns of microtransit. The framework can also help transit agencies with performance evaluation, regional transport strategies, and optimal vehicle dispatching.

TABLE OF CONTENTS

LIST OF FIGURES

LIST OF TABLES

EXECUTIVE SUMMARY

This research investigated the recent research in modeling the Mobility as a Service (MaaS) as an access mode to transit and found several studies that had researched various aspects of MaaS, but mostly as a stand-alone mode (e.g., Uber/Lyft) as opposed to an access mode to transit. Simultaneous with this research is a pilot project initiated by the Utah Transit Authority (UTA) in partnership with Via to provide an on-demand ride to light rail and commuter rail stations within a prescribed area. This service, often referred to as microtransit, is technology-enabled shared transportation that operates in between fixed-route transit and ride-hailing. The design of microtransit allows for integration into the current public transit system. Users often take advantage of microtransit to complete first mile/last mile connections to the larger transit system. Previous studies help deepen our understanding of microtransit and its dynamics. However, there is very little work concerning the spatio-temporal patterns of microtransit trips and the causal factors contributing to these patterns, especially under the impacts of COVID-19. This project leverages trip data from UTA's microtransit pilot for developing a methodological framework that unravels the spatio-temporal patterns of microtransit activities in the region. The framework utilizes eigendecomposition to uncover the rhythms and structures of microtransit trips. Using seven months of microtransit data, we constructed the spatiotemporal patterns of microtransit activities in pre- and post-COVID periods, respectively. Then, we systematically analyze how these patterns deviate from the average pattern in both periods and what possibly caused such variation. We use eigendecomposition to unravel the hidden temporal structures and k-clique percolation theory to explore the potential spatial communities formed in the service region. Also, for both periods, we intend to determine which locations are connected, how strong the connections are, what roles shared nodes (by different communities) play in different network structures, and how patterns evolve as COVID-19 progresses.

In the meantime, Utah Department of Transportation (UDOT) and Wasatch Front Regional Council (WFRC) have initiated a project to refactor the mode split model of the Wasatch Front Travel Model. The findings created under this research can be used to support this effort to refactor the mode split model.

1. INTRODUCTION

1.1 Problem Statement

The past few years have witnessed an explosive growth in new transportation modes. These new modes are leveraging digital technologies to offer efficient and convenient mobility services. The new mobility services include a wide variety of on-demand services, also referred to as "Mobility as a Service" (MaaS), ranging from short-term rentals of cars, bikes, and scooters to the peer-to-peer provisioning of transportation services. Although the share of these new mobility services is still small, a significant increase in their popularity can be expected due to reduced waiting times, competitive fares, and the promise of a one-seat ride. Transportation network companies (TNCs) such as Uber and Lyft are among the most successful of these mobility services. In 2018, 4 billion TNC rides were estimated in United States compared with 0.5 billion taxi rides. Uber operates in over 785 metropolitan areas worldwide and is estimated to have 110 million users across the world (Statista, 2020).

The success and growing popularity of the TNCs are largely due to a favorable regulatory environment, advancement of digital technologies, and innovative business models. Most TNCs are designed around smartphone platforms that allow travelers to request a ride at the push of a button, map estimated waiting time, and automatically pay by credit card. The platform estimates the travel cost based on travel distance, travel time, travel period, driver supply, and customer demand. Smartphone apps, treating drivers as independent contractors and requiring them to buy and maintain their vehicles and personal insurance, help to cut costs when compared with conventional taxi service. As a result, TNC fees are generally competitive with fares offered by traditional taxi service. Recently, new shared-ride services offered by TNCs, such as UberPool and LyftLine, are making TNCs competitive with traditional public transportation modes. One study estimated similar ridership for TNCs and public transit at the end of 2018 (Schaller, 2018).

Considering additional benefits and convenience that these new on-demand mobility services offer, they have the promise to significantly alter the transportation landscape as we know it. To date, most long-range transportation plans in Utah have not accounted for new mobility services and their impact on public transportation. This highlights the need for research to shed light on the impact of MaaS on transit ridership.

Microtransit, as a designated mode of MaaS, has been gaining popularity over the years. It is technology-enabled shared transportation that operates in between fixed-route transit and ride-hailing. It leverages rider aggregation and routing algorithms to group customers traveling within the service zone in similar directions in real time. Moreover, microtransit often expects customers to walk a short distance to common pick-up/drop-off locations. Thus, the service is transit-like but more nimble when compared with traditional public transit. As a technology-enabled on-demand service, microtransit shares many similarities with other services such as ride-hailing and paratransit. The platform collects requests from personal devices like smartphones then dynamically dispatches available vehicles to fulfill those requests. However, one substantial difference exists. The design of microtransit allows for integration into the current public transit system. Users often take advantage of microtransit to complete first mile/last mile connections to the larger transit system.

For microtransit, the global launch of pilot programs over the past five years (Haglund et al., 2019; Westervel et al., 2018) seeks to provide (and improve) first/last mile connections to fixed transit stops and stations, replace underperforming bus routes, provide coverage in areas without fixed-route service, and extend the hours of operation for existing bus services. Many studies analyze the overall performance of microtransit pilot programs (Haglund et al., 2019; Volinski, 2019) or microtransit vehicles (Ongel et al., 2019). For example, Haglund et al. (2019) systematically evaluated the performance of the *Kutsuplus*

pilot in Helsinki, Finland. The evaluation framework used aggregated measures and spatio-temporal metrics, including the average annual number of passengers, annual price per journey, user age class, and distribution of hourly departure/arrival trips for analysis. Volinski (2019) provided a case-based review and synthesis of more than 20 transit agencies that had implemented or intended to launch a microtransit service. This review included evaluations of underlying motivations, planning, design, marketing strategies, technology, and performance metrics. Ongel et al. (2019) evaluated the impacts of novel vehicle technologies on vehicle acquisition costs. This evaluation included lifecycle and end-of-life cost estimates for electric microtransit vehicles and conventional buses operating in Singapore.

Meanwhile, a new challenge has emerged for public transit. COVID-19, a novel coronavirus disease, became a global pandemic in 2020. Nearly 90% of the American adults reported that COVID-19 impacted their personal lives, and 44% of them claimed their lives had changed dramatically (Pew Research Center, 2020). Due to its collective nature, public transit has been hit even harder (Liu et al., 2020; Wilbur et al., 2020; Yi et al., 2021). In New York City, the average subway and commuter rail ridership declined by 80%, and bus ridership dropped by 50% (Gao et al., 2020a, 2020b) in the first week of July 2020 compared with 2019. In Washington, DC, subway and bus ridership declined by 90% and 75%, respectively, by the end of March 2020 (WMATA, 2020) compared with their typical values. In Utah, three major public transit modes – bus, FrontRunner, and TRAX – have witnessed a massive decline in total ridership upon the pandemic outbreak (Dillman & Posvistak, 2020). The week after the state of emergency was declared, average ridership declined by 56% compared with the previous week (Dillman & Posvistak, 2020). Similarly, there was a substantial downturn in microtransit use throughout Utah after the COVID-19 outbreak.

1.2   Objectives

The first objective of study is to create a methodological pipeline to effectively model MaaS as one of the first-mile/last-mile options for accessing transit. Transit access options incorporated into the current Wasatch Front model are park-and-ride, kiss-and-ride, and non-motorized). Addressing this important aspect of MaaS will give a more complete answer to the question of how this mode will affect future travel demand. The second objective of this study is to take a closer look at microtransit service, and to develop a modeling approach to capture such service, so that it can be applied within the planning modeling frameworks used for estimating travel demand.

This study is important for three reasons. First, because microtransit helps fill gaps between fixed-route systems and ride-hailing, it is essential to understand its underlying spatio-temporal patterns for a community. In short, does the service provide connectivity to the places that people want to go and when they want to get there? Second, the costs of delivering microtransit services can be substantial, and there are no guarantees that the service will attract riders. For example, the now-bankrupt *Bridj* service in Kansas City served only 1,480 riders during its year of operation, with the Kansas City Area Transportation Authority (KCATA) spending $1.5 million to subsidize the service. Considering that the first 10 rides were free for Bridj users, this translated into a subsidy of $1,000 per ride (Schmitt, 2018). Thus, there are real financial implications for communities offering microtransit services. Developing a framework that can provide the geospatial intelligence required for improving system performance is crucial for service sustainability. Third, while the influence of COVID-19 on microtransit is easily observable in Utah, there is no analysis of the overall effects. This research focuses on the underlying travel patterns associated with microtransit and their changes during the pandemic. Our findings could help transit agencies understand the decline in microtransit ridership and the relationships between the public health crisis and microtransit demand.

1.3   Outline of Report

The rest of the report is structured as follows. Chapter 2 summarizes the literature review. The proposed methodology, including the approach to modeling MaaS and our methodological framework for uncovering the microtransit activity pattern, are explained in Chapter 3. Chapter 4 details the data used in this study and their pre-processing. Finally, we offer results in Chapter 5 and conclude with a summary of our findings and key contributions of the study.

2. LITERATURE REVIEWS

Deployment of smartphone technologies in recent years has provided the technology platform for shared mobility services. MaaS as a viable mode is new and the research community has just begun to investigate the supply and demand characteristics of this mode. Several studies have investigated the impacts of user's characteristics, geographic context, and built environment factors on the adoption rate of MaaS. For example, Clewlow and Mishra (2017) conducted a comprehensive travel and residential survey in seven major U.S. cities with a representative sample of their urban and suburban populations. They found that the adoption rate of TNC services is approximately double among college-educated individuals compared to those without any college degree. Survey results revealed that 29% of Americans living in urban areas had used ride-hailing services in comparison with 15% of those living in suburban areas.

Kooti et al. (2017) reported while younger TNC riders tend to take frequent, shorter rides, older ones are more likely to take infrequent, longer rides.

In another study, Alemi et al. (2018) studied the lifestyle of TNC users to identify the factors impacting the adoption rate of ride-hailing services. They revealed that highly educated independent millennials who live in core urban areas without owning personal vehicles and without children have the highest adoption rate. They also reported a positive correlation between adoption rate of these services and the urbanization level of the neighborhood. Dias et al. (2017) estimated a bivariate ordered probit model to investigate the use of MaaS based on a survey dataset derived from a 2014-2015 Puget Sound Regional Travel Study. They found that users of such services are likely to be young, well-educated, higher-income, employed, and residing in higher density neighborhoods. The presence of children is found to reduce ride-hailing and carsharing usage among low and middle-income households. Results also revealed that households owning vehicles are less likely to use carsharing services and households residing in a high-density location are more likely to use both ride-hailing and carsharing services compared with their counterparts residing in low density areas. Several other studies also reported that ride-hailing users are more likely to own fewer cars (Conway et al., 2018; Hampshire at al., 2017).

In more recent studies, Yu and Peng (2019) indicated that population density along with road and sidewalk densities significantly impact the demand for TNC services. Xie et al. (2019) developed a nested framework to model the behavior of a local on-demand mobility service in the Boston-Cambridge region considering impacts of subscription services, service access, menu options and opt-out choices and their connections. The proposed framework is utilized to model the demand of the Tripod, an on-demand service that offers incentives for more energy efficient travel options through a real-time travel menu (Azevedo et al., 2018). They reported higher Tripod market penetration in lower income population segments. Moreover, Tripod's usage is found to be more associated with trips that have lower time constraints.

In summary early adopters of on-demand mobility services are found to be well-educated individuals living in urban areas. These services are considerably more popular among young adults who are heavy users of smartphone technology and related apps. Considering additional benefits that MaaS offers, it can draw a significant share away from conventional transportation modes (Haghighi et al., 2019). On the other hand, MaaS has the potential to increase transit ridership by filling first/last mile gaps in transit use. Several studies attempted to unveil whether MaaS competes with or complements transit use in urban areas. However, there is no consensus among researchers on the role that MaaS plays in serving public transportation. For example, while some studies reported that carsharing can complement the use of public transit (Firnkorn and Muller, 2011; Costain et al., 2012), another study showed that one-way carsharing can be a substitute for public transportation (Le vin et al., 2014).

Microtransit offers demand-responsive service to customers to initiate any trip start and end within a designated service area (FTA, 2021). This structure is similar to many mobility-based services, including bike-sharing and carsharing programs. Given the fact that mobile devices enable all these programs and one can retrieve a large amount of trip data from these services, there have been a myriad of studies to analyze spatio-temporal trip patterns (Alonso-González et al., 2018; Dong et al., 2018; Xu et al., 2019). For example, Xu et al. (2019) studied the spatio-temporal patterns of bike-sharing in Singapore. They associated the use patterns with built environment indicators such as floor area ratio (FAR) of residential buildings, FAR of commercial buildings, and land use mixture. In other work, Dong et al. (2018) studied both the service patterns and individual behavior patterns of internet-based ride-sharing services based on the record provided by DiDi, Inc. They applied a non-negative matrix factorization method and cluster analysis to study the spatial, temporal, and spatio-temporal elements of ride-sharing trips, as well as divisions of commuting styles and detour patterns. When it comes to microtransit analysis, Haglund et al. (2019) demonstrated the average journeys in specific periods during the day and the distribution of hourly departure/arrival trips based on the microtransit project *Kutsuplus*. While useful, this analysis was limited because it did not address the processes concerning underlying pattern formation. Similarly, Alonso-González et al. (2018) studied the distribution of generalized journey time across service areas in both aggregated and disaggregated levels using empirical data from a pilot program named "Breng flex" in the Netherlands. Again, while previous studies mainly focused on assessing how demand-responsive transport can benefit the current transportation network, we are not aware of any studies that use actual network data and analytics to examine the spatio-temporal patterns of microtransit usage. This research fills the gap by quantifying the evolving patterns of microtransit activities and elucidating the underlying reasons for such patterns.

3. METHODOLOGY

3.1 Approach to Modeling MaaS

This section summarizes various modifications to the current version of the Wasatch Front travel demand model to accommodate MaaS as a mode for accessing transit. Proposed modifications to the mode choice model would create a new modal option – MaaS – for accessing transit on the origin end of a trip (e.g., home-to-transit station) or on the destination end of a trip (e.g., transit station-to-work).

3.1.1 Mode Choice Modifications

In our previous research effort (UT-17.602), a new modal option was introduced to the motorized branch mode choice model representing MaaS (Figure 3.1). To represent MaaS as an access mode to transit, or microtransit, a new modal option is introduced in the transit access sub-nest. Within the transit access sub-nest, a MaaS option is added to the options already programmed into the mode choice model: walk/bike, park-and-ride, and kiss-and-ride. A simplifying assumption is that the MaaS access mode would be for fixed guideway modes only (LRT [shown], commuter rail [shown], BRT [not shown]).
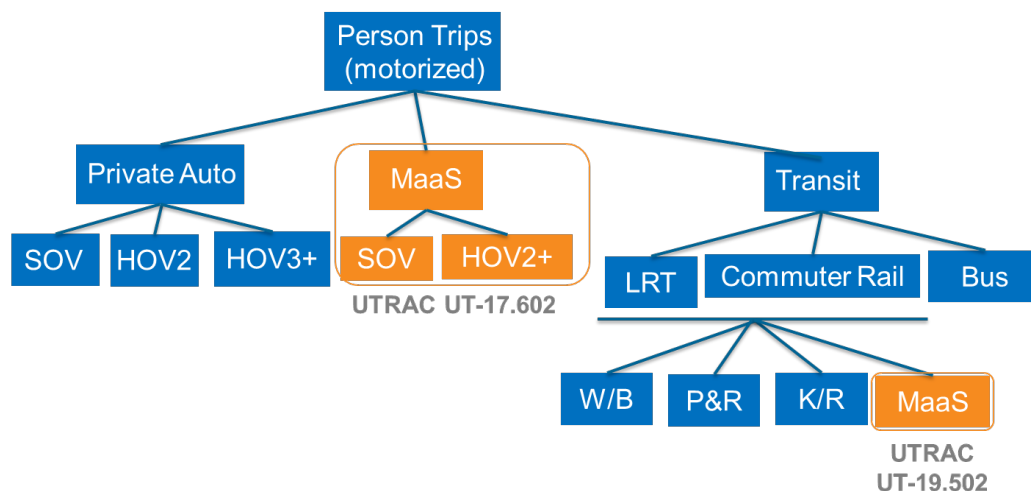
Figure 3.1 Schematic of modal options in the Wasatch Front travel model

The MaaS to Transit utility function would be very similar to the park-and-ride utility function, with additional time added to the trip for initial wait time (IWT). The MaaS to Transit utility function would also include a fare and possibly a new term reflecting the disutility of sharing a ride with strangers.

3.1.2 Steps to Implement Mode Choice Modifications

To implement the new access mode, "Maas to Transit," several steps are necessary, each of which involves a custom script to be called by the main travel model control script. These steps are depicted in Table 3.1.

Table 3.1 Steps to implement MaaS to Transit in the Wasatch Front travel model

Conduct for Origin and Destination End of Each Trip		Step 1	Create Drive Links for MaaS Access to Transit
		Step 2	Create Transit Skim to Include MaaS Drive Access Link
		Step 3	Include MaaS to Transit Nest for Selected Trip Types
		Step 4	Calculate Mode Utilities for Selected Trip Types
		Step 5	Revise Mode Choice Script Block to Include MaaS to Transit
		Step 6	Update Mode Choice Working Matrices Script Block - Final Output
		Step 7	Update Model Run Control Script

- Step 1: Create a drive access link to each transit station where MaaS to Transit is a viable mode. A simplifying assumption is to limit drive access links to fixed guideway transit only and to enforce a distance constraint whereby TAZ centroids outside a specified radius are considered impractical for this mode. A second simplifying assumption is for the drive access links to be calculated as straight-line distances (centroid to centroid).
- Step 2: Create a transit skim to include MaaS to Transit Access Link. This script determines the distance and cost for accessing transit stations using MaaS and assigns those costs to the overall transit trip.
- Step 3: This script incorporates MaaS to Transit within the Transit Nest for Selected Trip Types. The current script is written for the Home-Based-Work and Home-Based-Other trip types, though other trip types might be considered for MaaS to Transit.
- Step 4: Calculate Modal Utilities for Selected Trip Types. This script calculates the mode-specific utilities, which would include the utilities for transit trips using MaaS as an access mode. Typical inputs to modal utilities are travel time and travel fare. For MaaS to Transit, an Initial Wait Time would be added to the utility equation.
- Step 5: This script would calculate the revised mode choice to include MaaS to Transit if this sub-mode was determined to be the most competitive in the transit next.
- Step 6: This is the final Mode Choice output script, which would need to include MaaS to Transit trips.
- Step 7: The Cube model control script would need to be updated to run the six new scripts.

All steps would need to address MaaS to Transit on both the origin and destination end of each trip.

3.2 Spatiotemporal Microtransit Activity Pattern Analysis

3.2.1 Eigendecomposition

To uncover the spatiotemporal trip pattern for the microtransit program, we developed a methodological framework to delineate the variation and the homogeneity/heterogeneity in trips across spatial and temporal dimensions. Specifically, we employ eigendecomposition to achieve this. Eigendecomposition is well suited for this as it is good at uncovering hidden structures of spatiotemporal patterns. Compared to other variation extraction methods, such as factor analysis and analysis of variance, eigendecomposition is advantageous because it does not assume any distribution, error term, or underlying statistical model. Eigendecomposition generates a series of directional vectors (i.e., principal components [PCs]) based only on the data, each of which best explains variation while remaining orthogonal to other components. One orders the PCs by the amount of variance that they explain. For example, the first PC explains the most variance, the second PC explains the second most variance, and so on. Eigendecomposition is often used in statistical modeling to reduce dimensionality by projecting the data into a few PCs. One can also use eigendecomposition to explore the inherent variation within datasets. Our study uses

eigendecomposition to unravel the deviation from (or resemblance of) the average pattern of microtransit usage within the service area in both pre- and post-COVID periods.

We assume that microtransit arrival and departure patterns differ from each other. Therefore, all trips are further categorized into four groups: (a) pre-COVID departure; (b) pre-COVID arrival; (c) post-COVID departure; and (d) post-COVID arrival. During the study period, over 800 pick-up and drop-off locations resulted from 31,168 unevenly distributed trips within the service area after merging nearby locations. For example, among the 892 trip pick-up locations, the most popular pick-up location generated 2,633 trips, while over 50% of pick-up locations generated less than 12 trips each. To ensure unbiased analysis, we use traffic analysis zones (TAZ) to aggregate the pick-up and drop-off locations and uncover the trip patterns' geographic dimensions. Among the 163 TAZs within the service area, those that produced over 87 trips (median) and attracted over 85 trips (median) are labeled as active TAZs and used in this study. These 77 TAZs accounted for more than 91.7% of the total microtransit trips; 16,522 trips occurred pre-COVID, and 12,062 trips occurred post-COVID.

Using pre-COVID departure trips as an example, we illustrate the basic structure of our eigendecomposition. We formulate departure trips as follows:

$$N = \begin{pmatrix} n_{1,6} & \cdots & n_{1,21} \\ \vdots & \ddots & \vdots \\ n_{77,6} & \cdots & n_{77,21} \end{pmatrix} \tag{1}$$

In matrix N, $n_{i,j}$ represents the total number of departure trips originated from TAZ i ($1 \leq i \leq 77$) and in hour j ($6 \leq j \leq 21$). We ensure that the 16 variables (6:00 – 22:00) contribute equally to the variance maximizing exercise during eigenvalue decomposition by normalizing matrix N by dividing each row by its summation N'. Correspondingly, $n_{i,j}'$ represents the hourly percentage of departure trips during the pre-COVID period. Note that:

$$\sum_{j=6}^{j=21} n_{i,j}' = 1 \quad \forall i \in [1,77] \tag{2}$$

We then average hourly departure trips across all TAZs to obtain the average temporal pattern of departure trips within the service area. Let d_j denote the average departure trip percentage in TAZ j.

$$d_j = \sum_{i=1}^{i=77} n_{i,j}' \ / \ 77 \ j \in [6,21] \tag{3}$$

D = $\{d_6, d_7, d_8, \ldots, d_{21}\}$ represents the average temporal pattern of microtransit activities across the 77 active TAZs. We measure the deviation of microtransit trips from this average pattern with matrix M, which we construct subtracting d_j from column j of matrix N:

$$M = \begin{pmatrix} n_{1,6}' - d_6 & \cdots & n_{1,21}' - d_{21} \\ \vdots & \ddots & \vdots \\ n_{77,6}' - d_6 & \cdots & n_{77,21}' - d_{21} \end{pmatrix} \tag{4}$$

We perform eigendecomposition by first calculating the covariance matrix, S, where:

$$S = \frac{1}{n-1} M^T M \tag{5}$$

As a result, we can derive eigenvectors $v_6, v_7, v_8, \dots, v_{21}$ with the corresponding eigenvalues $\lambda_6, \lambda_7, \lambda_8, \dots, \lambda_{21}$ where $v_i s$ are all column vectors. Also, the principal components that explain a large portion of the total variance (summation of eigenvalues) can help interpret the overall patterns of microtransit activities. Thus, by applying eigendecomposition, we can uncover the spatio-temporal patterns of microtransit activities at different locations and examine how they deviate or resemble the average pattern in pre-COVID and post-COVID periods.

3.2.2 K-clique Percolation

k-clique percolation is a variant of the traditional percolation theory. Percolation theory aims to discover how networks behave when removing nodes or links. It is a method to gradually break down large networks into smaller connected clusters or sub-networks. This method works because the removal of key nodes or links in any network creates disconnections. Generally, percolation theory starts with a weighted or unweighted graph and ends at a graph containing only isolated nodes. The nature of percolation theory makes it suitable for identifying strongly connected subgraphs in the network, also known as community detection (Fortunato, 2010). Most community detection algorithms, including percolation, classify one node into one cluster or community *only*. However, k-clique percolation identifies overlapping communities by assigning specific nodes to *multiple* communities. This methodological attribute is essential for understanding microtransit because many first-mile/last-mile trips will make the transit station a pivot node that belongs to multiple communities. This local transport context is the primary reason we use k-clique percolation in this research. Moreover, the concept of k-clique is a good analogy to individuals' microtransit travel patterns. People frequently travel between a limited number of locations within a service region.

Figure 3.2 illustrates a 7-node unweighted and undirected network to highlight how k-clique percolation works. There are three key definitions:
>   Definition 1. k-clique is a fully connected or complete subgraph of k nodes.
>   Definition 2. Adjacent k-cliques are k-cliques that share exactly k-1 nodes.
>   Definition 3. A k-clique community is the union of all possible adjacent k-cliques.
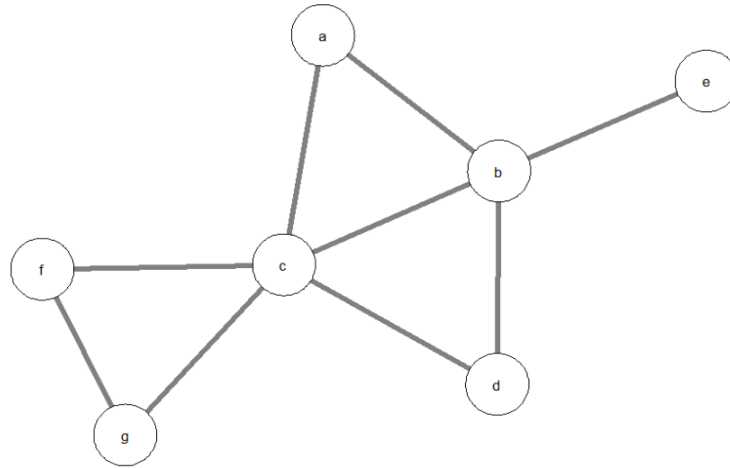

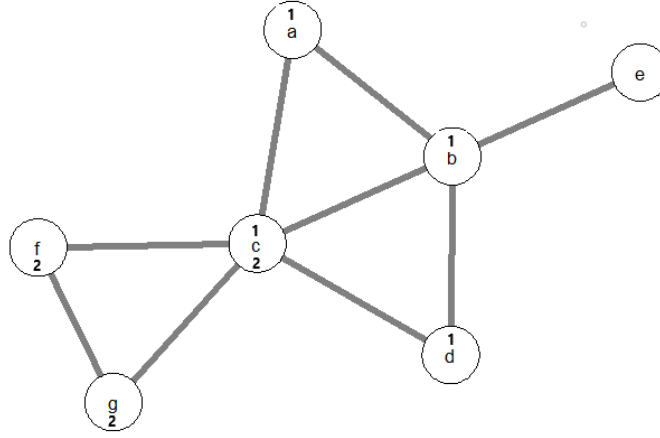**Figure 3.2** An unweighted and undirected graph with 7 nodes

Figure 3.3 Result of 3-clique percolation

The first step of *k*-clique percolation is to identify *k*-cliques. Here we choose *k* = 3 for illustration. There are three 3-cliques in the example network: a – b – c, b – c – d, and c – f – g. The next step is to identify possible adjacent *k*-cliques which make up communities. Figure 3.3 highlights the results with each node corresponding to its assigned community (by number). For example, node c belongs to both community 1 and 2, while node e does not belong to any community. For the weighted graph, there exists one additional intermediate step. In traditional percolation theory, a probability threshold determines whether two nodes are connected or not. Similarly, for the *k*-clique percolation method, we define an *intensity* threshold to determine whether a *k*-clique can be part of adjacent *k*-cliques. Specifically, intensity is a measure of the strength of connectivity of a clique. We define intensity as the geometric mean of the link weights of a certain *k*-clique:

$$\boldsymbol{Intensity} = \left(\sum_{1 \leq m \leq n \leq k} \boldsymbol{W_{m,n}} \right)^{\frac{2}{k(k-1)}} \tag{6}$$

We denote the intensity threshold by *I,* and we do not consider cliques whose intensity is below the threshold value for adjacent cliques. In Figure 3.4, we detail a weighted and undirected graph. The number on the link represents the link weight. Among the three 3-cliques identified in Figure 5, two of them have an intensity value of 0.187 (a-b-c and c-g-f), and one of them has an intensity of 0.1 (c-b-d) according to Equation (6). When one sets *I* as 0.01, all three cliques survive the threshold. According to definition 2, clique a-b-c and c-b-d are considered adjacent. Thus, there are two communities detected in the network. One contains node a, b, c, and d, and the other contains nodes c, f, and g, where node c belongs to both communities and node e is an isolated node (Definition 3). When $I = 0.18$, cliques a – b – c and c – f – g survive, but we eliminate clique c-b-d. Likewise, cliques a-b-c and c-g-f now make two separate communities while nodes e and d are isolated nodes. When $I = 0.2$, no clique survives. This type of network structure measurement is how *k*-clique percolation works for given values of *I* and *k*. However, an outstanding challenge remains – namely, determining optimal values for *k* and *I*.
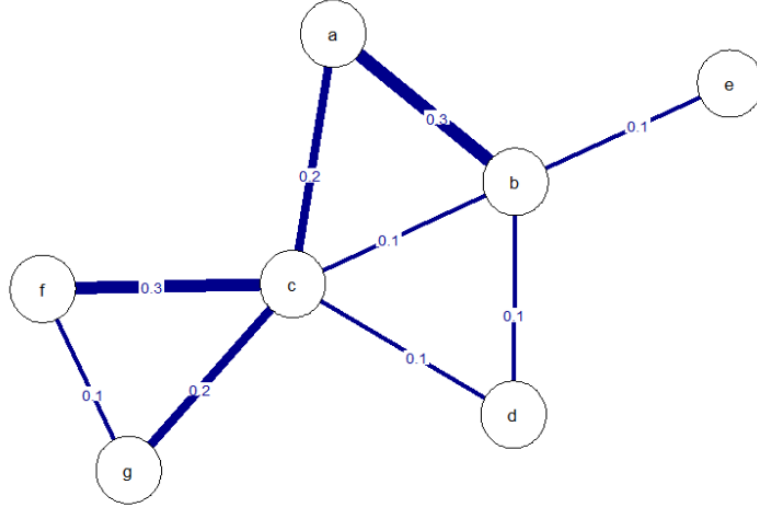
Figure 3.4 Weighted graph with 7 nodes

The criterion of choosing k and I is to find the most highly structured communities possible. Although different k and I values can generate various optimal subgraphs, there is still a need to set a global rule such that the overall structure and pattern can be analyzed. Derenyi et al. (2005) highlight one way to do this. Specifically, as one continues to remove links in a graph, a gigantic component containing a large portion of the existing nodes will eventually emerge. Thus, a rule of thumb for determining I for each k (typically 3 to 6) is to choose an I that is smaller than the value that allows the emergence of the gigantic component (Derenyi et al., 2005; Pallas et al., 2015). This value of I is considered the critical point for this network at a specific k. One can argue that the size of communities at the critical point follows a power-law. One can estimate this critical point of I by calculating the ratio between the size (number of nodes) of the largest community and the second-largest community. In Pallas et al. (2005), the ratio is set to 2 so that there is neither a gigantic community that slanders the details of the network nor are there too many small communities making the network poorly structured.

Moreover, to further study the connectivity of local cohesiveness, we apply the concept of a clustering coefficient (Barrat et al., 2004). As a measurement of inner-connectivity in the network, one can apply the clustering coefficient in two ways: 1) the clustering coefficient of a single node and 2) the average clustering coefficient of all nodes in the network. For weighted networks, one can use the clustering coefficient to evaluate the importance of clustered structures based on the aggregated link weights of the local triplets. In this instance, a triplet refers to three nodes connected by either two (e.g., open triplet, examples: a-b and b-c in Figure 3.4) or three (e.g., closed triplet, example: a-b, b-c and a-c in Figure 3.3) undirected links. Closed triplets are known as a 3-clique. In a network where one denotes a complete node set as N, the formula for calculating clustering coefficient for node i is:

$$C_i = \frac{1}{s_i(n_i - 1)} \sum_{j,k} \frac{(w_{ij} + w_{ik})}{2} a_{ij} a_{jk} a_{ik} \quad j, k \in N \quad (7)$$

Where, a_{ij}, a_{jk} and a_{ik} are binary indicators implying connection ($a_{ij}, a_{jk}, a_{ik} = 1$) or disconnection ($a_{ij}, a_{jk}, a_{ik} = 0$). w_{ij} is the weight between node i and j. n_i is the degree of node i defined as $n_i = \sum_j a_{ij}$. s_i corresponds to node strength, which measures the network property of node i in terms of the weights obtained by extending the definition of node degree n_i. We define this as:

$$s_i = \sum_j a_{ij} w_{ij} \qquad (8)$$

C_i accounts for all triplets formed around i in terms of average link weight. We normalize this by $\frac{1}{s_i(n_i - 1)}$ so that $0 \leq C_i \leq 1$. Larger values for C_i, indicate more cohesiveness for nodes around i. This structure means that the nodes around i are more tightly connected. We define the average clustering coefficient C_{avg} is defined as:

$$C_{avg} = \frac{\sum_i C_i}{|N|} \quad i \in N \qquad (9)$$

One can use C_{avg} to estimate the level of network overlap. Higher values of C_{avg} suggest more overlap.

In the context of microtransit activities, our goal is to identify communities in pre-COVID and post-COVID periods to examine the pattern within each period and how the pattern evolves. Again, we treat each pick-up or drop-off location as nodes in the network. Since the customers using microtransit programs tend to travel between a limited number of locales multiple times, the outflow and inflow of most nodes are almost equal to each other. Hence, we construct the network as an undirected and weighted graph. We measure link weights as the ratio between the trip count on each link and the maximal trip count across all links. We apply k-clique percolation to the built network to uncover the underlying communities and how communities evolve. The preliminary analysis for both pre-COVID and post-COVID periods suggests a value of $k = 3$ will provide a good baseline for measurement. When $k \geq 4$, the number of k-cliques is very limited, and more than 75% of the nodes became isolated even when $I = 0$. Also, less than 4% of the nodes will survive when reaching the critical point. In other words, $k \geq 4$ eliminates a vast portion of the network before structure detection. After we fix k to 3, we explore a range of values for I to reveal different levels of information. When $I = 0$, one can treat the system as an unweighted network since any 3-cliques can survive the threshold. In this case, we fully preserve the topological structure. However, as we increase the values of I, cliques with less weight will continue to dissipate. Only the cliques with larger weights (more trips) will remain in the network.

4. DATA

4.1 Data Source

UTA partnered with Via transportation to launch a microtransit pilot program beginning November 2019 in South Salt Lake. Salt Lake County funded the project. This on-demand, shared-ride pilot is designed to expand access to the transit service throughout the service zone, improve mobility for all users, and provide a quality customer experience. UTA conducted this pilot to see whether microtransit provides a valuable and cost-effective service and whether a future deployment of microtransit service is possible. The project experienced early success, meeting most goals and objectives before the COVID-19 pandemic, including ridership, cost, customer rating, and vehicle hours traveled.

The microtransit program serves about 65 square miles in the cities of Bluffdale, Draper, Herriman, Riverton, and South Jordan in Utah. Figure 4.1 shows the service area, including seven TRAX and FrontRunner stations, which are the main components of UTA's rail system. The program provides a corner-to-corner service in the region from 6:00 to 22:00 on weekdays only. It allows riders to be picked up and dropped off within a walkable distance (on average 0.1 miles) from their chosen origins and destinations.

Figure 4.1 Service area of UTA on Demand with Via (Source: *UTA on Demand,* 2021)

The trip data used in this research contain features related to each trip request, including rider ID, pick-up/drop-off coordinates, pick-up/drop-off time, trip duration, trip distance, number of passengers, ride cost, payment type, request source, customer ratings, and wheelchair accessibility. We present the detailed description of the full feature set in Table 4.1. The study period spans January 1, 2020, to July 31, 2020, encompassing 31,199 trips from 1,569 unique users. Among these 31,199 trips, there are 2,472 unique pick-up points and 2,317 unique drop-off points. Apart from the seven TRAX and FrontRunner stations in Figure 4.1, common pick-up/drop-off locations include apartment complexes, single-family houses, supermarkets, churches, educational institutions, private companies, and personal businesses (e.g., pet stores and liquor stores), among others.

Table 4.1 Feature descriptions of raw data

Features	Levels of Measurement	Units	Range
Rider ID	Nominal		
Pick-up lat	Interval	Decimal degree	[40.464, 40.568]
Pick-up long	Interval	Decimal degree	[-112.071, -111.83]
Drop-off lat	Interval	Decimal degree	[40.463,40.568]
Drop-off long	Interval	Decimal degree	[-112.071, -111.83]
Pick-up time	Interval		[01/01/2020 08:24:00, 07/31/2020 21:00:00]
Drop-off time	Interval		[01/01/2020 08:48:00, 07/31/2020 21:06:00]
Trip duration	Ratio	Minute	[0, 437.817]
Trip distance	Ratio	Mile	[0.077, 11.104]
Num. of passengers	Ratio		[1, 5]
Ride cost	Ratio	Cent	[0, 1250]
Payment type	Nominal		UTA ticket, Apple Pay, Credit card, Free, Google Pay, Ride credit, Waived
Request source	Nominal		App, Call center
Customer rating	Ordinal		1, 2, 3, 4, 5
Wheelchair accessibility	Nominal		0: wheelchair-accessible vehicle 1: non-wheelchair-accessible vehicle

4.2 COVID-19 in Utah

The first confirmed COVID-19 case in Utah was reported on March 6, 2020. The patient was aboard the Grand Princess cruise ship and later diagnosed (Utah Department of Health, 2020). This event, however, does not fully represent the community spread of COVID-19 in Utah. Figure 4.2 presents the daily average confirmed COVID-19 cases in each month and daily average microtransit trips in different periods between January 1 and July 31, 2020. Figure 4.2a demonstrates how COVID-19 progressed within the service area and the entire state of Utah, respectively. The service area as mentioned above consists of the cities of Bluffdale, Draper, Herriman, Riverton, and South Jordan. Figure 4.2b shows the daily average microtransit trip counts within the study periods (January, February, March 1 – March 13, March 14 – March 31, and April through July). We split March into two periods to highlight the comparison before and after the state of emergency declaration.

As seen in Figure 4.2a, at the state level, the daily average confirmed COVID-19 cases have increased dramatically since March 2020, with the largest increase during June 2020. However, within the service area, during March through May, the confirmed cases remained at a comparatively low level. Nevertheless, the cases increased sharply in June and July, suggesting a wide community spread of COVID-19.

If we compared the trend of microtransit trips in Figure 4.2b, there is some consistency. Before March 13 (state of emergency declaration date), daily average microtransit trips increased steadily as the user base of the pilot program was growing. However, between March 14 and March 31, the daily average trip count dropped dramatically from 325.4 trips per day to 94.4 trips per day. The trip count reached its lowest level in April and May, at 73.4 trips per day and 80.3 trips per day, respectively. The trend in March through May suggests the significant impacts of COVID-19 on microtransit activities. Users were

less inclined to use microtransit or stopped using it completely. Trip counts started to increase slightly in June and July, marking the recovery of microtransit activity or overall public transit usage. In the meantime, as we observed in Figure 4.2a, a notable increase in COVID-19 cases happened during the same period in the service area.
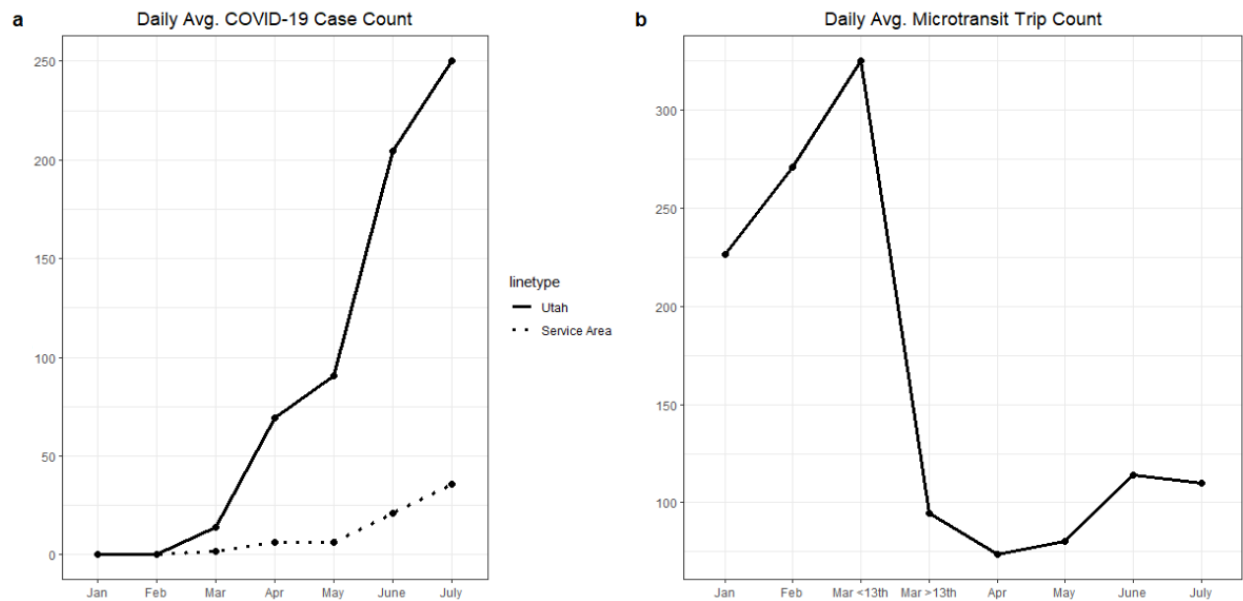

Figure 4.2 Trends of COVID-19 cases and microtransit trips

4.3 Preliminary Processing

Given the nature of corner-to-corner service, the actual origin of a trip is most likely within a walkable distance from the pick-up point (available in the trip data). The same applies to the drop-off locations. That said, the trip data show a wide dispersion of pick-up and drop-off points, where multiple points might lead to identical origins and destinations. Thus, this research applies hierarchical agglomerative clustering (HAC) to separately aggregate nearby pick-up and drop-off points to facilitate subsequent analysis (Murtagh & Contreras, 2012). Agglomerative hierarchical clustering is a standard clustering method based on the distance of clusters. It is a bottom-up approach that assigns each unit to its cluster at the beginning. Then clusters are iteratively merged with their closest neighbors.

When applying HAC, one must determine the pruning parameter – height – representing the number of iterations (merging clusters). Larger values for height (iterations) yield fewer clusters. For this analysis, we select a value of 300 so that the average distance within clusters is close to 0.1 miles. This value is the average walking distance assumed by Uber pool service (Pachal, 2018). Figures 4.3 and 4.4 highlight the distributions of pick-up and drop-off locations, respectively.

(a)   (b)

Figure 4.3 Distribution of trip pick-up locations (a) before and (b) after merging

(a)   (b)

Figure 4.4 Distribution of trip drop-off locations (a) before and (b) after merging

After merging pick-up and drop-off locations, we further divide the dataset into two periods, with a cut-off date of March 13, 2020, corresponding to the declaration of the COVID-19 outbreak as a national emergency in the United States. This date and data partition helps distinguish the potentially heterogeneous spatio-temporal patterns as a result of the pandemic. Upon screening of missing values, the pre-COVID period consists of 17,980 trips, and the post-COVID period consists of 13,188 trips.

5.   RESULTS AND DISCUSSIOIN

5.1   Eigendecomposition

There are 16,522 pre-COVID trips and 12,062 post-COVID trips in the 77 active TAZs used for analysis. These counts translate to an average of 229.5 and 86.2 trips per day, respectively. Such daily usage of microtransit demonstrates a sharp decrease in activities since the outbreak of COVID-19. Figure 5.1 presents the overall temporal patterns (sum of each hour) for departure and arrival trips in pre- and post-COVID regimes, respectively. Both regimes show a two-peak distribution, one in the morning (7:00 – 9:00) and one in the evening (16:00 – 18:00). Moreover, the departure vs. arrival trip patterns are very similar (with a small time lag) because the service region is limited, and the average trip duration is around 10 minutes. Apart from the overall decline in microtransit activities, it is interesting to note the pronounced drop in the morning peak (7:00 – 8:00) after the COVID-19 outbreak.
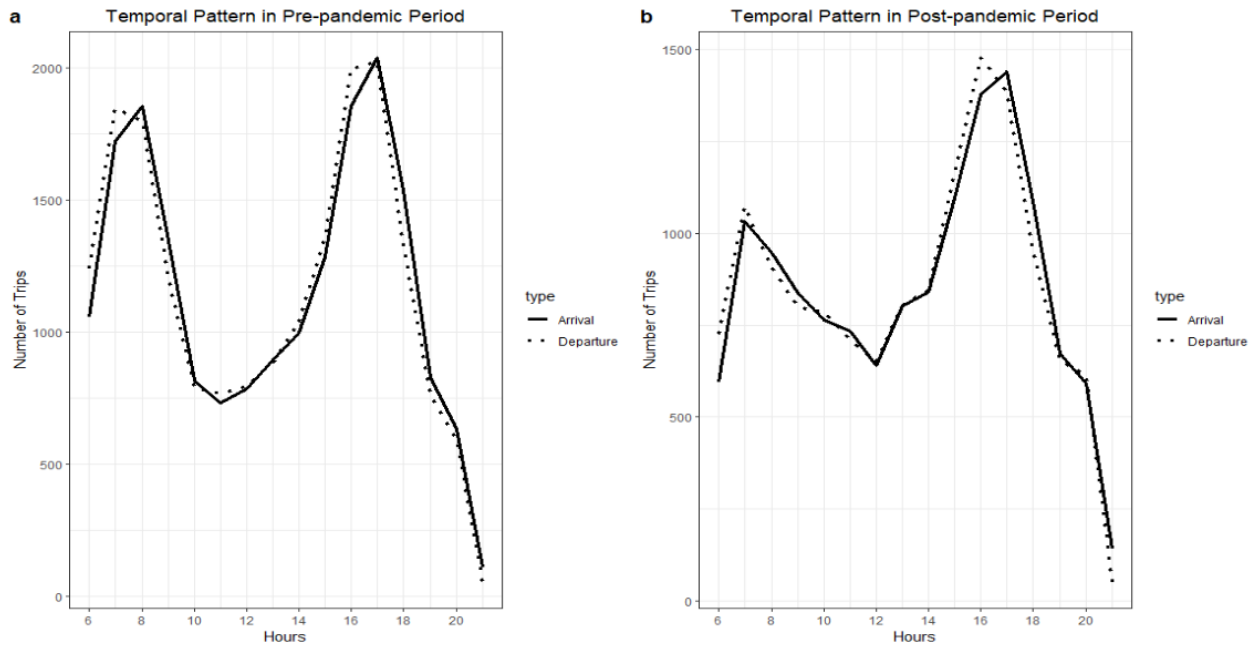
Figure 5.1 Distribution of edges by the number of trajectories

Table 5.1 shows the total variance and the respective portions of variance explained by the first four PCs. Here, we apply three empirical rules to decide upon a suitable number of PCs (Jolliffe, 2002; Xu et al., 2019):

1. The chosen PCs cumulatively explain more than 70% of the total variation.
2. The eigenvalues of the chosen PCs are larger than 0.7 times the average eigenvalue.
3. The chosen PCs are to the left of the elbow points of scree plot, which shows the eigenvalues for each PC.

Given these guidelines, we use the first four PCs for further analysis.

Table 5.1 Summary of eigendecomposition

	Total Variance	PC1	PC2	PC3	PC4
Pre / Departure	0.088	37.4%	17.7%	11.8%	10.1%
Pre / Arrival	0.073	36.4%	12.9%	11.1%	9.5%
Post / Departure	0.098	23.9%	16.1%	15.5%	10.4%
Post / Arrival	0.096	27.5%	15.8%	12.5%	9.1%

Table 5.1 shows that the first four PCs explain more than 60% of the total variation for all four trip categories. While the results are largely homogeneous, each of the four categories displays its own temporal structure. For example, the variance of pre-COVID trips is smaller than post-COVID trips, generally speaking. This result suggests that microtransit usage is more consistent in the pre-COVID period, but it is more diverse (from place to place) in the post-COVID period.

Also, in the pre-COVID period, the variance of departure trips is significantly larger than that of arrival trips (by 21%). However, in the post-COVID period, their variance is quite similar. This result suggests a higher diversity in temporal patterns for departure trips when compared with arrival trips, pre-COVID. Nevertheless, this temporal signature disappeared in the post-COVID period. One possible explanation for this is that drop-off locations are often more connected (for trip purposes) than pick-up locations. This finding suggests that TAZs with similar social functions tend to generate similar microtransit usage patterns. As a result, the total variance is lower.

In this research, first-mile/last-mile trips are important. This type of trip accounts for more than 58% of total trips in the pre-COVID period, resulting in a more uniform arrival pattern. However, after the COVID-19 outbreak, the percentage of first-mile/last-mile trips continues to decrease. For example, in July, 2020, the relative number of trips dropped to 29%. Meanwhile, trip purposes have become much more diverse, making the variance of arrival trips close to departure trips.
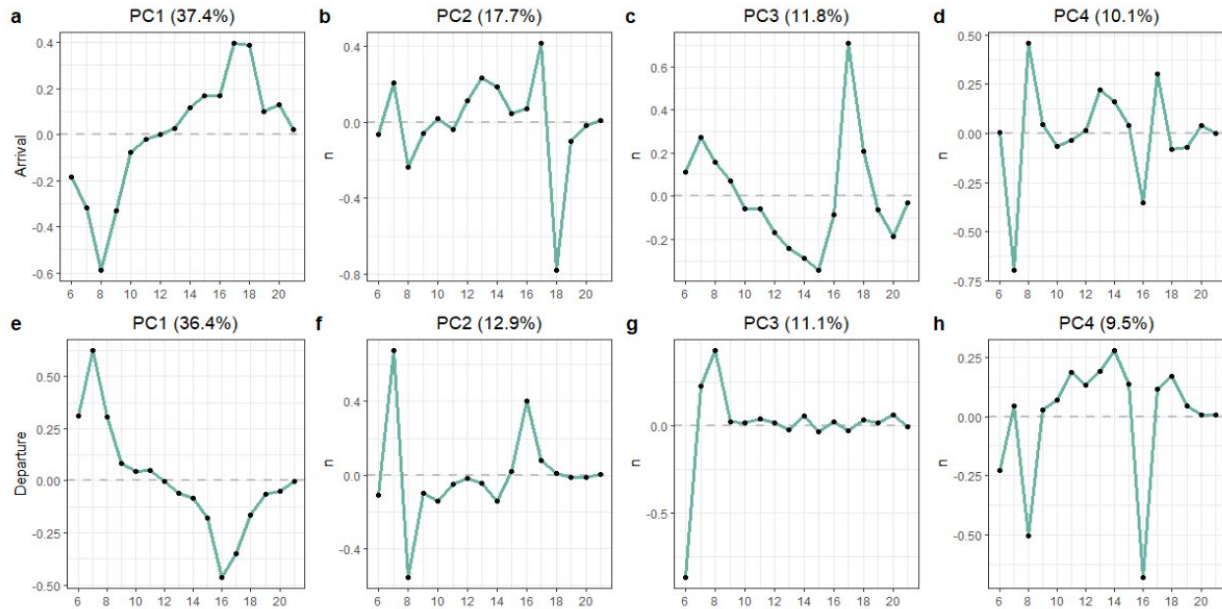
Figure 5.2 Eigendecomposition of pre-COVID arrival and departure trips

The first several PCs can help summarize the spatio-temporal patterns of microtransit activities. Figure 5.2 displays the first four PCs for pre-COVID trips. In Figure 5.2, the x-axis represents the 16 input variables that correspond to each hour when the service is in operation, and the y-axis demonstrates the

loadings of the first four PCs associated with all the input variables. In other words, the y-axis is the coefficient of the linear combination between PCs and input variables. For example, PC1 of pre-COVID arrival trips explains 37.4% of the total variation and shows a clear two-peak pattern at 7:00 – 10:00 and 17:00 – 19:00 (Figure 5.2a). This result suggests that microtransit activity during these two time periods varies considerably, especially when compared with the uniformity found in other periods. Figure 5.2e also suggests that PC1 for departure trips explains 36.4% of the total variation and has a similar two-peak pattern, yet the graph shifts slightly to the left. The two-peak periods are 6:00 – 9:00 and 16:00 – 18:00. Such a pattern is consistent with the morning and evening peaks of transit usage, indicating that both arrival and departure trips have the most diversified spatio-temporal patterns during these two peak periods.

Of note are the results from Figure 5.2a. In this instance, the coefficients of PC1 have opposite signs in the morning and evening peaks. This result suggests that if a TAZ attracts more microtransit trips during 7:00 – 9:00, then arrivals trips are likely lower in that TAZ during 17:00 – 19:00. In fact, of the top five TAZs that attract most trips in the morning peak, four of them attract a limited number of trips in the evening peak. The pattern holds true for departure trips as well. If more people departed certain TAZs from 16:00 – 18:00, fewer customers would tend to depart from those TAZs from 6:00 – 9:00.

While the coefficients of PC1 support these results, PC2, PC3, and PC4 combine to explain 39.6% of the variation for arrival trips and 33.5% variation for departure trips. This explanatory power means that there are other significant temporal patterns that PC1 cannot explain (by itself) and that many TAZs do not follow the patterns shown by PC1. For example, PC2 explains 17.7% of the total variation for arrival trips, suggesting a notable shift in the morning and evening peaks (Figure 5.2b). Further, Figure 5.2b suggests that in some TAZs if more patrons arrive from 17:00 – 18:00, fewer customers will arrive at those TAZs from 18:00 – 19:00. Figure 5.2f highlights a similar pattern for departure trips. The variation of temporal patterns peaks during 7:00 – 8:00 and 8:00 – 9:00, yet in opposite directions. Moreover, PC3 and PC4 each explains around 10% of the total variation for both arrival and departure trips. The proximity of variance explained by PC1, PC2, PC3, and PC4 suggests a variety of underlying temporal patterns in pre-COVID microtransit activities, which, to some extent, uncovers the diversity of trip purposes.

To deepen our understanding of the causal mechanisms for the patterns displayed in Figure 5.2, we focus on the temporal pattern of first-mile/last-mile trips. In this study, the first-mile/last-mile trips either start from or end at any transit station identified in Figure 4.1. Figure 5.3 shows the percentage of first-mile/last-mile trips over total trips that start in each hour for the pre-COVID and post-COVID periods, respectively. The average value in Figure 10 is the average percentage of total first-mile/last-mile trips over total trips for the pre-COVID and post-COVID periods, respectively. The percentage of first-mile/last mile-trips of both arrival and departure trips peaks between 6:00 – 9:00 and 16:00 – 19:00. This result means that many patrons travel to or from transit stations during those time periods. It is important to note that the first-mile/last-mile trip patterns are quite similar pre- and post-COVID. In other words, although there is an overall reduction (from 58.07% to 47.88%) in percentage, first-mile/last-mile trips still account for a large portion of the total trips. One can observe the same peaks in Figure 5.2a and Figure 5.2e. This pattern implies that when the percentage of first-mile/last-mile trips is high, the variation in travel patterns is more extensive and vice versa. As we further examine PC3 and PC4 of arrival and departure trips, please note that the variation peaks between 6:00 – 9:00 and 16:00 – 19:00. These windows are when the percentage of first-mile/last-mile trips is above average (Figure 5.3). It indicates that PC1, PC3, and PC4 all capture part of the variation caused by first-mile/last-mile trips.
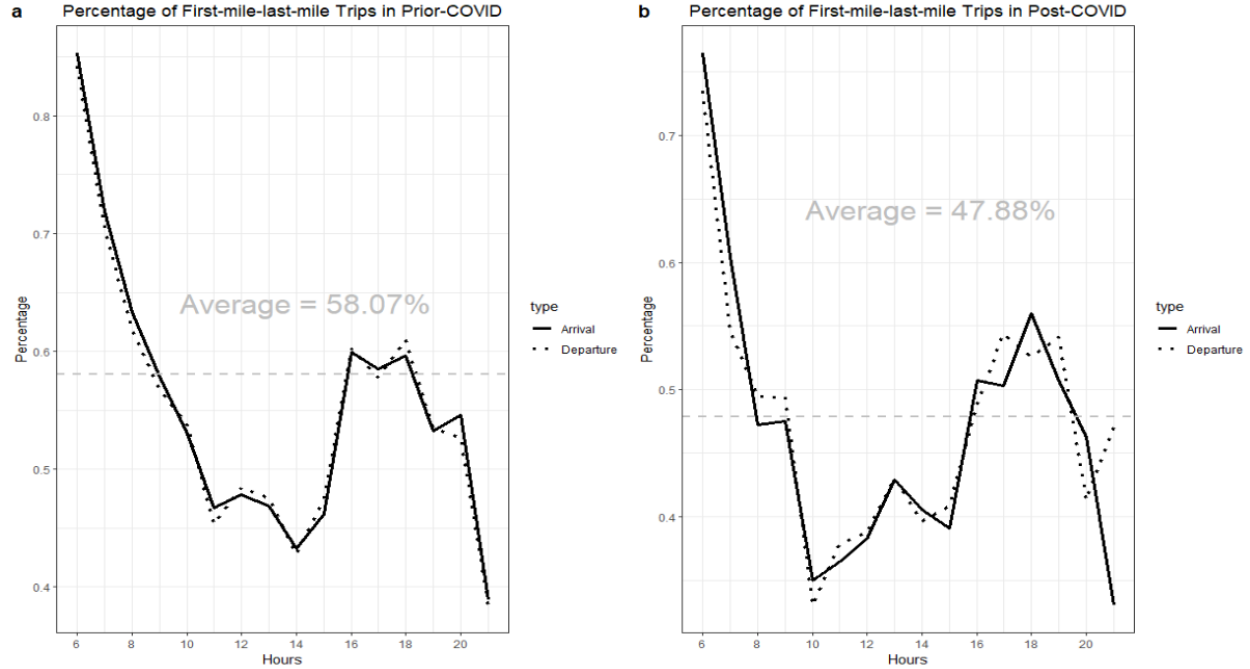
Figure 5.3 Percentage of first-mile/last-mile trips

Figure 5.4 presents the eigendecomposition of post-COVID trips. One focus of the eigendecomposition is to study how COVID-19 has altered the temporal patterns of microtransit activities. For example, Figure 5.4a and Figure 5.4e illustrate a similar two-peak pattern for arrival and departure trips. For arrival trips, the largest variation occurs from 8:00 – 9:00 and 18:00 – 19:00. For departure trips, the peak periods are 6:00 – 7:00 and 16:00 – 17:00. Thus, one might suggest that specific patterns emerged after the outbreak of COVID-19. However, the variance explained by PC1 for arrival and departure trips decreased from 37.4% and 36.4% to 27.5% and 23.9%, respectively. This decrease in variance explained by PC1 suggests that the temporal patterns of post-COVID trips are more diverse. Also, different patterns can be found based on the PCs. For instance, PC2 for post-COVID arrival trips demonstrates a different one-peak pattern. Specifically, for some TAZs, trip arrival is most active and diverse from 13:00 – 14:00 (Figure 5.4b). That said, PC2, PC3, and PC4 do not exhibit such a pattern for pre-COVID arrival trips. The difference between the two eigendecomposition results suggests a substantial pattern transition after the outbreak of COVID-19.

Based on the results of eigendecomposition, the first-mile/last-mile trips are likely to be the primary source of variance, which PC1 explains in both pre- and post-COVID periods. Moreover, transit-dependent users remain inelastic despite the threats brought by COVID-19 (Figure 5.3). However, the patterns are mutable. For example, there are reductions in microtransit activity along with first-mile/last-mile trips. In addition, there is a dispersive trend for pick-up and drop-off locations and the emergence of new travel patterns. In the next section, we analyze the coordinates of pick-up and drop-off locations to detect underlying community structures and compare the temporal patterns of these locations to the service area averages.
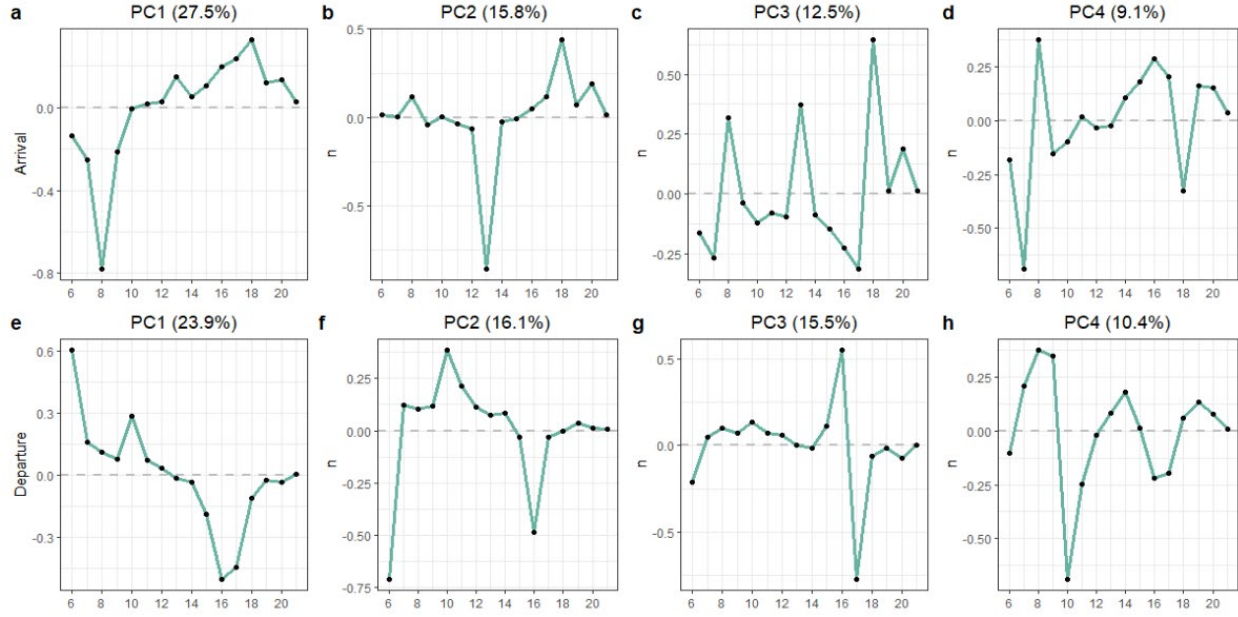
Figure 5.4 Eigendecomposition of post-COVID arrival & departure trips

5.2 K-clique Percolation

5.2.1 Pre-COVID Period

There are 17,980 trips in the pre-COVID period from 1,235 different users in 1,163 pick-up and drop-off locations. The maximum number of trips is 348, while the minimum number is 1. We first vary I (intensity thresholds) to see how communities progress. We present the evolving pattern of communities with increasing values of I in Figure 5.5. Specifically, Figure 5.5a displays the total number of communities in response to changes in I. Figure 5.5b demonstrates the size ratio of the largest community to the second-largest community. For higher values of I, community formation decreases. This type of pattern is not always monotonic. For example, when I increases, cliques with lower levels of intensity will disappear. Simultaneously, these eliminations will dissolve large communities into smaller ones. For instance, in Figure 5.5b, the ratio is well above 2 when I is small, indicating a gigantic community, with a few small communities containing a minimal number of nodes. The formation of a gigantic community suggests a wide connection across the service region, apart from a few pick-up or drop-off locations. The vertical dashed line in Figure 5.5 highlights the "critical" point, which is detailed in Chapter 3. Specifically, when I increases from 0, fewer 3-cliques remain in the network. Until I reaches 0.031, the gigantic community that contains most of the nodes breaks down into two medium-sized communities with a ratio of 4.05. Thus, we identify $I = 0.031$ as the critical point for the pre-COVID microtransit network.
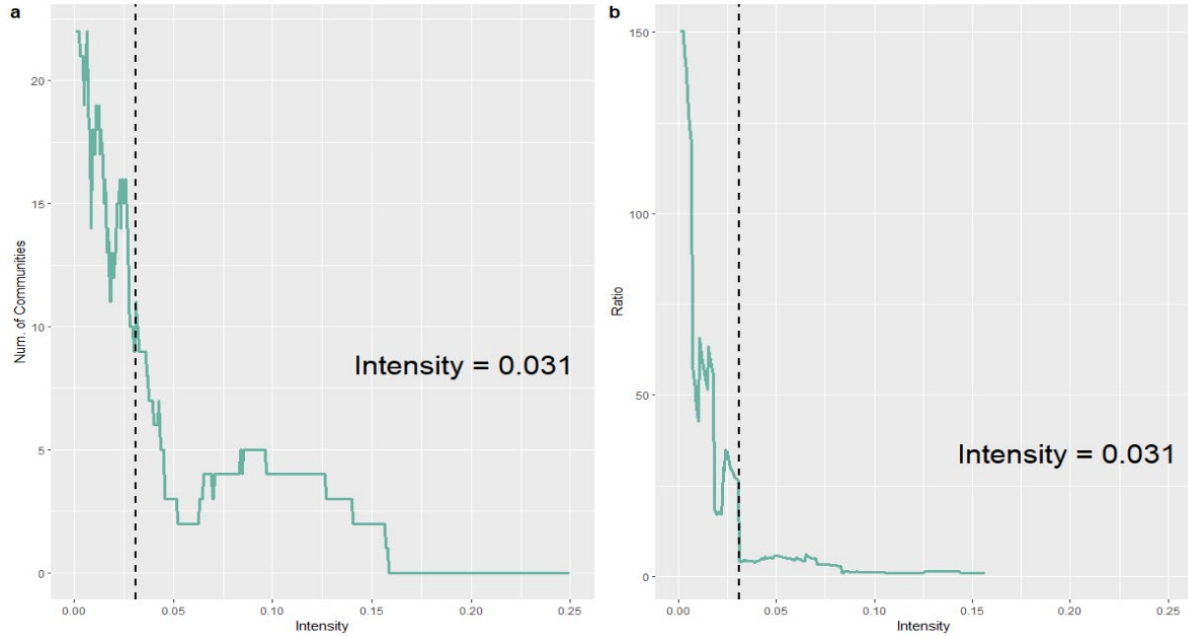
Figure 5.5 Community summary under different intensity thresholds: (a) the number of communities; and (b) the size ratio of the largest community to the second-largest community

We further explore the characteristics of communities using 10 unique values for *I*: 0, 0.031, 0.047, 0.063, 0.079, 0.095, 0.111, 0.127, 0.143, and 0.159. *I* = 0 represents the point when all 3-cliques remain in the network without any isolated node. *I* = 0.031 is the critical point. When *I* = 0.159, only one community remains in the network. The remaining seven values are interpolated at an increment of 0.016 from *I* = 0.031 to *I* = 0.159. We present these results in Table 5.2, along with the corresponding community attributes. When multiple communities have the same number of nodes, we break the tie by selecting the community with the highest trip rate. We select the two largest communities for illustrative purposes because their size ratio is an important indicator of community structure. Also, the two largest communities account for a majority (≥ 85%) of the total trips. In Table 5.2, *Size* represents the number of nodes contained in the community. *Trips* are the indicator of the total amount of trips captured by the community. *FMLM* trips stand for first-mile/last-mile trips with a calculated percentage of total trips. *Users* are the unique number of customers who appeared across the trips. *Avg. Trips* equal to trips divided by users. *Duration* is the average trip length of all trips in the unit of minutes in that community.

22

Table 5.2 The result of 3-clique percolation for the pre-COVID period

I	Community	Size	Trips	FMLM Trips (% of total trips)	Users	Avg. Trips (trips/person)	Duration (minutes)
0	1	601	15735	9818 (62%)	1039	15.1	10.3
	2	4	13	11 (85%)	5	2.6	12.3
0.031	1	81	4930	4330 (88%)	361	13.7	9.6
	2	20	699	564 (81%)	65	10.8	8.2
0.047	1	42	3128	2835 (91%)	237	13.2	8.8
	2	8	441	400 (91%)	38	11.6	8.6
0.063	1	26	2240	1992 (89%)	156	14.4	9.0
	2	6	336	319 (95%)	35	9.6	7.7
0.079	1	15	1410	1338 (95%)	117	12.4	9.4
	2	5	291	231 (79%)	16	18.2	6.0
0.095	1	5	471	466 (99%)	51	9.2	12.2
	2	4	321	306 (95%)	28	11.5	7.3
0.111	1	4	321	306 (95%)	28	11.5	7.3
	2	4	244	189 (77%)	11	22.18	6.2
0.127	1	4	321	306 (95%)	28	11.5	7.3
	2	3	409	409 (100%)	49	8.3	13.0
0.143	1	4	321	306 (95%)	28	11.5	7.3
	2	3	409	409 (100%)	49	8.3	13.0
0.159	1	3	239	224 (94%)	14	17.1	6.72
	2						

In general, the evolution of communities follows a hierarchical structure. As values of I increase, 3-cliques with lower values of intensity begin to disappear. However, when $I = 0$, all 3-cliques survive. Again, this turns the network into an unweighted and undirected graph. This scenario means that one can consider any link as only connected or disconnected. The communities detected when $I = 0$ are a good reflection of the connectivity across the region. There are 22 communities in the network, and the largest one is a gigantic community that contains 601 nodes. The remaining communities contain only 3 or 4 nodes (Table 5.2). It is worth mentioning that the remaining 22 communities include 626 nodes in total, leaving 537 nodes forming no 3-cliques. In other words, 537 nodes do not belong to any clique. These isolated nodes demonstrate a commuting pattern for *specific individuals*. In other words, trips concerning the 537 pick-up or drop-off locations are user-centric. The locations are not likely to be shared across different users.

When $I = 0.031$ (critical point), the gigantic component breaks down into two medium-sized communities (81 and 20). In this scenario, the community structure is strong, maximum information is present, yet it displays a distinguishable pattern. For example, Figure 5.6 and Figure 5.7 demonstrate the spatial distribution of the two largest communities and the shared nodes when $I = 0.031$. Figure 5.6 suggests that the spatial pattern of the network includes a distribution of nodes from the entire region, accounting for six of 85.7% (6 of 7) of the major transit stations. However, a new spatial pattern emerges in Figure 5.7. The second-largest community contains a congregation of 20 nodes from the west side of the service area. The corresponding trips gravitate to the Daybreak Parkway station, with 81% of trips being first-mile/last-mile trips. This result suggests that the pick-up and drop-off locations surrounding Daybreak Parkway

station maintain a connection, which provides valuable information for possible vehicle dispatching and routing optimization.
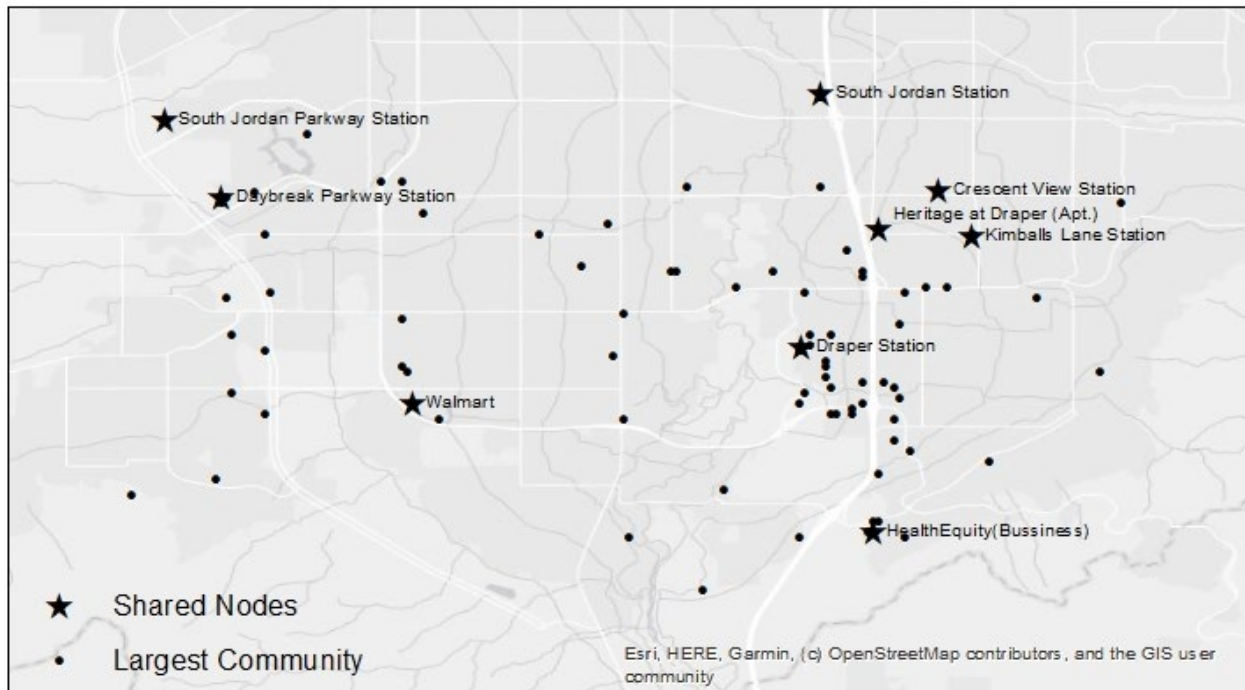

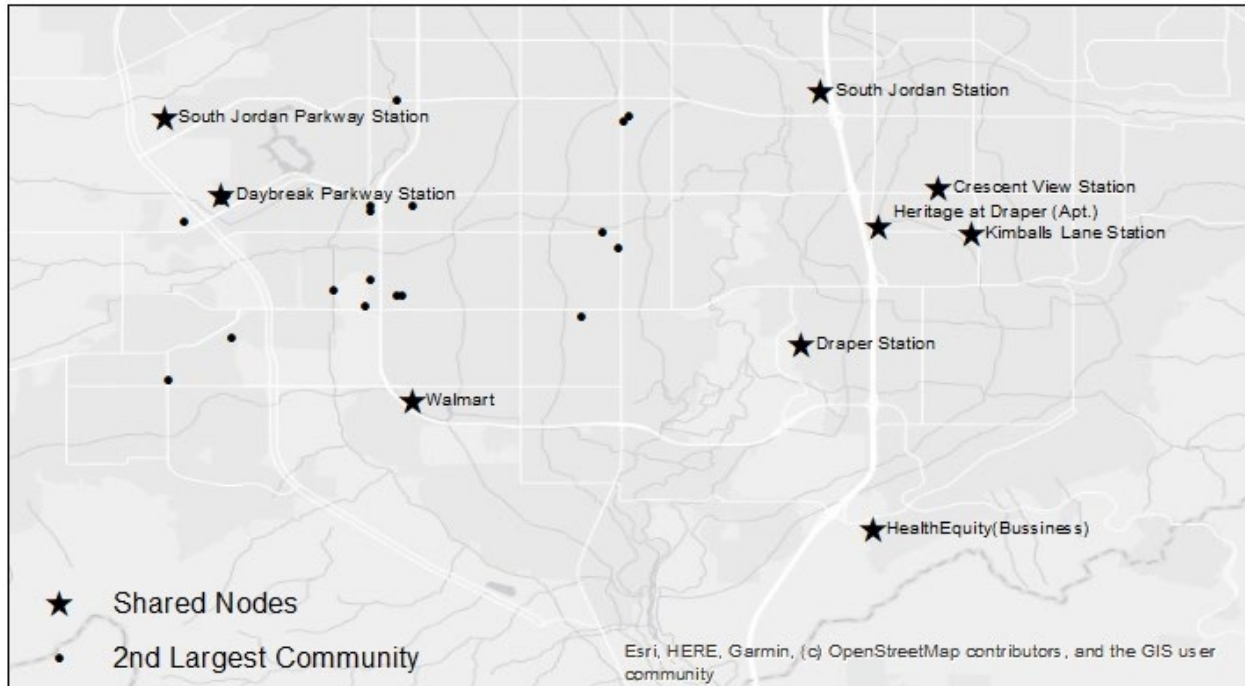**Figure 5.6** The largest community and shared nodes when $I = 0.031$ in the pre-COVID period

Figure 5.7 The second-largest community and shared nodes when $I = 0.031$ in the pre-COVID period

Section 5.1 explored how first-mile/last-mile trips contribute to the spatio-temporal patterns of microtransit activities. Similarly, we observe a dominant percentage of first-mile/last-mile trips for different Is in Table 5.2. When $I = 0$, the largest community has 15,735 trips, with 62% being first-mile/last-mile trips, slightly higher than the average (58.07%). However, only 35% of trips occur outside of network communities, with the majority connecting isolated nodes. This difference suggests that first-mile/last-mile trips enhance the connectivity between popular pick-up and drop-off locations. Trips connecting isolated nodes are more user-specific and less dependent on transit. Further, at the critical point, first-mile/last-mile trips account for a large portion of the total trips in both the largest and second-largest communities with a minimum of 77% and a maximum of 100% (Table 5.2). Clearly, first-mile/last-mile trips play a crucial role in connecting the entire region.

We also explore 3-clique communities, their overlap, and levels of connectivity. We use the average clustering coefficient, C_{avg}, to measure local community cohesiveness. Without any processing, the C_{avg} of the original network is 0.169. This high value suggests significant overlap between communities in the pre-COVID period. Also, it means that when two communities overlap, they are likely to overlap with each other. Figure 5.8 presents this trend graphically. As values of I increase, there is a removal of isolated nodes and 3-cliques with lower I values. This trend results in increasing values of C_{avg}, although there is some fluctuation. The results suggest that popular (i.e., large trip counts) pick-up and drop-off locations are tightly connected, resulting in high C_{avg}.

Community structure is also important to consider, especially at the critical point. When $I = 0.031$, there are nine shared nodes with clustering coefficients ranging from 0.017 to 0.32. Note that six of these nine nodes with the lowest clustering coefficient correspond to major transit stations, while the top three correspond to an apartment, a private company, and a supermarket (Figure 5.6 and Figure 5.7). The average clustering coefficient of the six transit stations is 0.0275, well below C_{avg} (0.169) of the original network. Moreover, among the six transit stations, Draper Station has the largest nodal degree, yet the smallest clustering coefficient, 0.017. In contrast, Kimballs Lane Station has the lowest nodal degree yet the largest clustering coefficient, 0.049. A similar pattern emerges for the top four nodes that are not transit stations. All have smaller nodal degrees and larger clustering coefficients, with a maximal of 0.32. This result suggests a different distribution pattern between transit stations vs. non-transit stations. For transit stations, a hub-and-spoke pattern best describes the system surrounding them. In short, traffic travels along the links connecting different nodes to a central distribution center (transit stations). However, those nodes themselves are not well connected. For apartments, private companies, and supermarkets, the underlying pattern better corresponds to a point-to-point structure. In these instances, riders can use microtransit to travel directly between those locations without going through a central hub.
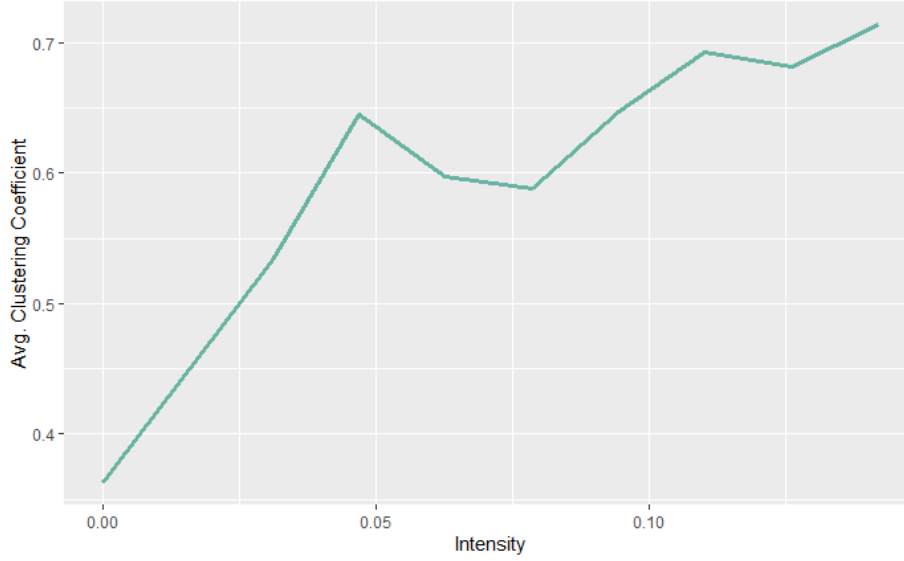
Figure 5.8 The average clustering coefficient at different *I*

5.2.2 Post-COVID period

There were 13,188 trips by 794 unique users (334 new) between 1,040 pick-up and drop-off locations in the post-COVID period. The maximum number of trips is 221, while the minimum number is one. We present the results of the 3-clique percolation in Figure 5.9. In Figure 5.9a, the same decreasing pattern with fluctuations is apparent. In Figure 5.9b, the ratio is well above 2 when *I* is small, but the value has dropped slightly because of less microtransit activity in general. The vertical dashed line stands for the critical point in the post-COVID period.
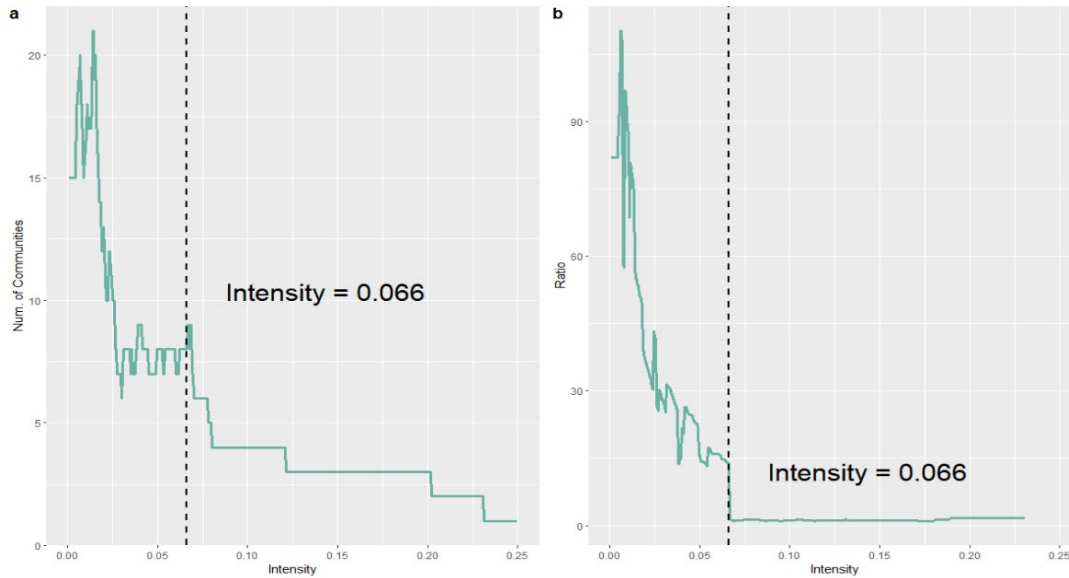

Figure 5.9 Community summary under different intensity thresholds in the post-COVID period: (a) the number of communities; and (b) the size ratio of the largest community to the second-largest community

26

The characteristics of communities is further explored at 10 values of I in the same manner: 0, 0.066, 0.087, 0.108, 0.129, 0.150, 0.171, 0.192, 0.213, 0.234. Table 5.3 displays the results.

Table 5.3 The 3-clique percolation for the post-COVID period

I	Community	Sizes	Trips	FMLM Trips (% of total trips)	Users	Avg. Trips (trips/person)	Duration (minutes)
0	1	492	10948	5737 (52%)	610	17.9	9.5
	2	6	9	0 (0%)	2	4.5	8.4
0.066	1	25	1549	1520 (98%)	82	18.9	6.3
	2	18	1042	919 (88%)	81	12.9	24.3
0.087	1	11	820	809 (99%)	38	21.6	6.3
	2	11	817	712 (87%)	50	16.3	5.3
0.108	1	9	750	748 (99%)	30	25.0	6.3
	2	7	630	621 (99%)	35	18	5.3
0.129	1	7	630	621(99%)	35	18.0	5.3
	2	6	517	516 (99%)	24	21.5	6.3
0.150	1	6	601	600 (99%)	34	17.7	5.3
	2	5	468	468 (100%)	18	26.0	6.3
0.171	1	6	601	600 (99%)	34	17.7	5.3
	2	5	468	468 (100%)	18	26.0	6.3
0.192	1	5	551	550 (99%)	30	18.4	5.3
	2	3	162	162 (100%)	13	12.5	5.2
0.213	1	5	551	550 (99%)	30	18.4	5.3
	2	3	157	157 (100%)	11	14.3	7.2
0.234	1	5	551	550 (99%)	30	18.4	5.3
	2						

When $I = 0$, the network yields a gigantic component that contains 492 nodes while the remaining communities contain six or fewer nodes and 530 nodes in isolation. Compared with the pre-COVID period, there are more isolated nodes (51% vs. 46%). This result indicates that the user-centric pattern has become more distinct after the outbreak of COVID-19.

When $I = 0.066$ (critical point), two medium-sized communities (25 and 18) emerge from the gigantic network. Figure 5.10 and Figure 5.11 present the spatial distribution of both and the shared nodes. There are some significant spatial changes worth noting. First, the spatial distributions of the two communities became less distinct. The largest community contains Draper Station, Draper Town Center Station, and Crescent View Station. The second community contains Draper Station, Crescent View Station, South Jordan Station, and Daybreak Parkway Station. The major takeaway here is that both communities span around major transit stations across the region. Also, their *Sizes* and *Trips* (in Tables 5.2 & 5.3) are similar, suggesting that these two communities are equally important in the post-COVID period.

In addition, for all values of I, the number of users has decreased. This result is likely due to the overall decline in microtransit activity. However, the average number of trips per user increased compared with the pre-COVID period (Tables 5.2 and 5.3). There are two possible explanations. One is that less frequent users might have stopped using microtransit due to pandemic concerns. The other is that those who depend on microtransit remain riders (e.g., transit dependents and essential workers). Aside from these

differences, similarities also emerge. For example, many trips remain in the network for different values of *I,* and the first-mile/last-mile trips account for a large percentage of total trips for both periods.

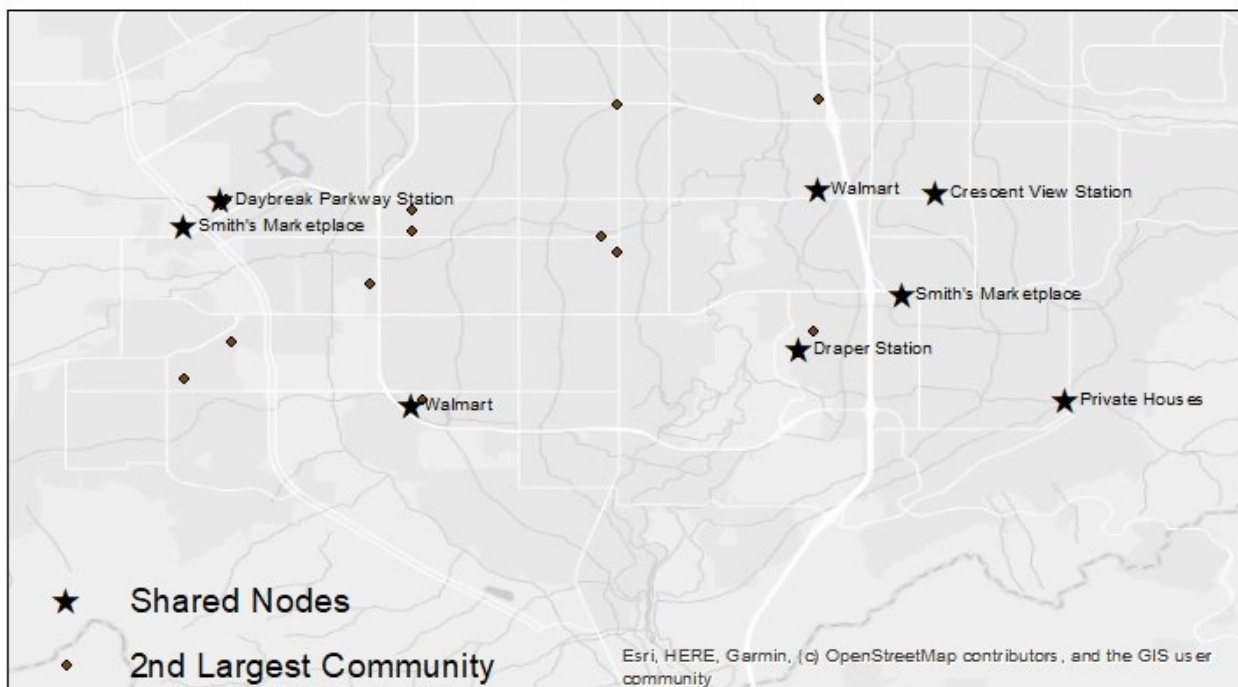**Figure 5.10** The largest community and shared nodes when $I = 0.066$ in the post-COVID period

Figure 5.11 The second-largest community and shared nodes when $I = 0.066$ in the post-COVID period

We are also interested in how the overlapping pattern changes. Figure 5.12 presents the average clustering coefficients for different values of I. The C_{avg} of the original network decreased from 0.169 (pre-COVID) to 0.129 (post-COVID). This result indicates that the level of network overlap decreased. At the critical point, we identify eight shared nodes. The three with the lowest clustering coefficient are transit stations with a minimal clustering coefficient of 0.029 (Draper Station) and a maximal clustering coefficient of 0.041 (Crescent View Station). The top five nodes contain four supermarkets and one residential node (Figure 18) with a minimum coefficient of 0.073 and a maximal coefficient of 0.124. The hub-and-spoke distribution for transit stations and point-to-point distribution for supermarkets and residential locations were also present in the post-COVID period.
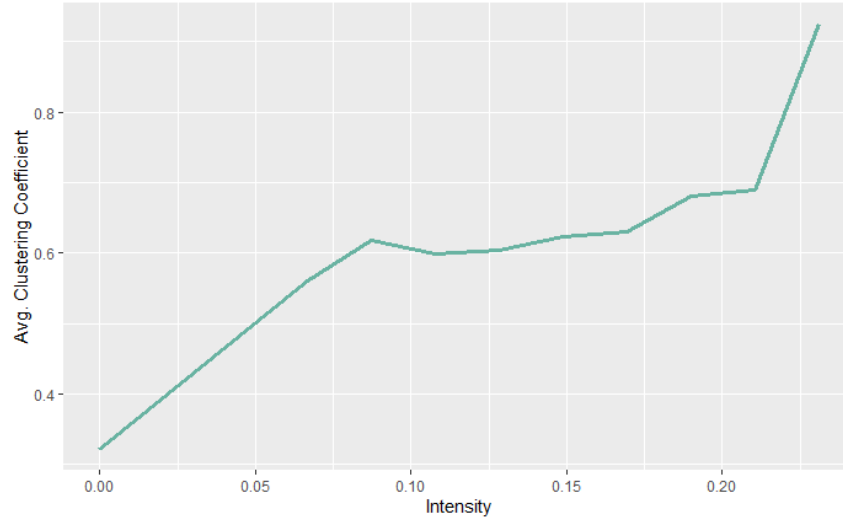

Figure 5.12 The average clustering coefficient at different I

6. CONCLUSIONS

MaaS is a new mode of travel that encompasses several concepts. As applied in this research, MaaS refers to an on-call service that would give patrons access to fixed rail transit stations. Modeling MaaS as an access mode to transit involves seven steps, described in this research, which must be conducted for both the origin (accessing transit on the origin end of the trip) and the destination (accessing the final destination from the transit stop on the destination end of the trip) end of the trip. Within the current framework of the Wasatch Front travel model, including MaaS-to-transit involves custom scripting using the Cube software scripting language.

To further explore one of the newest variations of MaaS, we unravel the spatio-temporal structures of microtransit activities utilizing empirical data from a pilot program in the Salt Lake City, Utah, area, UTA Via. The results compare microtransit activity during pre- and post-COVID periods, highlighting how some use patterns persist and change after the outbreak.

The results of the eigendecomposition suggest that first-mile/last-mile trips declined, but the hourly distribution remained nearly identical. This finding suggests transit dependency for many riders. However, several new patterns emerged. Specifically, the explanatory power of PC1 decreased. This finding suggests a temporal dispersion trend for microtransit activity after the pandemic. Furthermore, by focusing on first-mile/last-mile trips, our results suggest that a higher percentage of first-mile/last-mile trips leads to greater variation for PC1. This result means that first-mile/last-mile trips can be the major source of variation in both periods.

We further apply k-clique percolation to identify the communities in two networks (pre-COVID and post-COVID). We vary threshold values of *I* for each network. As *I* increases, the gigantic component begins to break down into medium-sized communities. During this process, the results suggest that first-mile/last-mile trips account for most of the total trips captured by the network.

The application of a clustering coefficient revealed that network overlap decreased after the COVID-19 outbreak. Interestingly there was an emergence of two distinct communities, pre- and post-COVID. The communities surrounding transit stations take the form of hub-and-spoke systems, with transit stations serving as traffic distribution centers while the surrounding nodes are disconnected. For other popular locales, connections are more dispersed, demonstrating a point-to-point distribution style.

This work aimed to reconstruct and understand the spatio-temporal patterns of microtransit activity in portions of Salt Lake City, Utah. The framework is generalizable and can provide additional insights for UTA Via as it grows or inspires applications to pilot programs in other cities. By understanding the patterns and possible causal factors for microtransit network development, use, and underlying spatio-temporal patterns, one can enhance the transferability of microtransit programs without additional cost. Furthermore, spatio-temporal structures of microtransit usage reveal that the usage is uneven. For example, the connection between certain regions is significantly stronger than that of other places. Also, the two-peak temporal pattern demonstrates many variations resulting from first-mile/last-mile trips. Understanding these structures of microtransit activity can help with possible customer segmentation and vehicle dispatching for all microtransit programs. Lastly, by comparing results between pre- and post-COVID periods, it is possible to inform transit agencies on people's behavioral changes and the evolution of their travel patterns to guide operational strategy adjustments further.

REFERENCES

Alemi, F., Circella, G., Handy, S., and Mokhtarian, P. (2018). "What influences travelers to use Uber? Exploring the factors affecting the adoption of on-demand ride services in California." *Travel Behaviour and Society*, 13, pp. 88-104.

Alonso-González MJ., Liu T., Cats O., Van N., and Hoogendoorn, S. (2018). "The Potential of Demand-Responsive Transport as a Complement to Public Transport: An Assessment Framework and an Empirical Evaluation." *Transportation Research Record*. 2672(8): 879-889.

Azevedo, C.L., Seshadri, R., Gao, S., Atasoy, B., Akkinepally, A.P., Christofa, E., Zhao, F., Trancik, J., and Ben-Akiva, M. (2018). "Tripod: sustainable travel incentives with prediction, optimization, and personalization." In Transportation Research Board 97th Annual Meeting.

Barrat A., Barthélemy M., Pastor-Satorras R., and Vespignani, A. (2004). "The architecture of complex weighted networks." *Proceedings of the National Academy of Sciences, 101 (11)*, 3747-3752.

Clewlow, R. R., and Mishra, G. S. (2017). "Disruptive transportation: The adoption, utilization, and impacts of ride-hailing in the United States." Retrieved from https://itspubs.ucdavis.edu/wp-content/themes/ucdavis/pubs/download_pdf.php?id=2752.

Conway, M., Salon, D., and King, D. (2018). "Trends in taxi use and the advent of ridehailing, 1995–2017: Evidence from the US National Household Travel Survey." *Urban Science*, 2(3), p.79.

Costain, C., Ardron, C., and Habib, K. N. (2012). "Synopsis of users' behaviour of a carsharing program: A case study in Toronto." *Transportation Research Part A: Policy and Practice, 46*(3), 421-434.

Dias, F.F., Lavieri, P.S., Garikapati, V.M., Astroza, S., Pendyala, R.M., and Bhat, C.R. (2017). "A behavioral choice model of the use of car-sharing and ride-sourcing services." Transportation, 44(6), pp.1307-1323.

Dillman, M., and Posvistak, C. (2020). "COVID-19 and Public Transportation in Utah." *Inquiry of the Public Sort.*

Dong Y., Wang S., Li L., and Zhang, Z. (2018). "An empirical study on travel patterns of internet based ride-sharing." *Transp. Res. Part C: Emerg. Technol*., 86, 1–22.

Federal Transit Administration (FTA). (2021).

  https://www.transit.dot.gov/regulations-and-guidance/shared-mobility-definitions

Firnkorn, J., and Müller, M. (2011). "What will be the environmental effects of new free-floating car-sharing systems? The case of car2go in Ulm." *Ecological Economics, 70*(8), 1519-1528.

Fortunato, S. (2010). "Community detection in graphs." *Physics Reports*, vol 486, issues 3–5, 75-174.

Gao J., Wang J., Bian Z., …, and Ban, X. J. (2020). "The Effects of the COVID-19 Pandemic on Transportation Systems in New York City and Seattle, USA." arXiv preprint arXiv:2010.01170.

Gao, J., Bernardes, S. D., Bian, Z., Ozbay, K., and Iyer, S. (2020). "Initial Impacts of COVID-19 on Transportation Systems: A Case Study of the US Epicenter, the New York Metropolitan Area." arXiv preprint arXiv:2010.01168.

Haglund N., Mladenović M.N., Kujala R., Weckström C., and Saramäki, J. (2019). "Where did Kutsuplus drive us? Ex post evaluation of on-demand micro-transit pilot in the Helsinki capital region." *Res. Transp Bus. Manag*, 32, 100390.

Hampshire, R., Simek, C., Fabusuyi, T., Di, X., and Chen, X. (2017). "Measuring the Impact of an Unanticipated Disruption of Uber/Lyft in Austin, TX. Available at SSRN: https://ssrn.com/abstract=2977969 or http://dx.doi.org/10.2139/ssrn.2977969

Kooti, F., Grbovic, M., Aiello, L.M., Djuric, N., Radosavljevic, V., and Lerman, K. (2017). "Analyzing Uber's ride-sharing economy." *In Proceedings of the 26th International Conference on World Wide Web Companion* (pp. 574-582). International World Wide Web Conferences Steering Committee.

Liu L., Miller H. J., and Scheff, J. (2020). "The impacts of COVID-19 pandemic on public transit demand in the United States." *Plos one, 15(11)*, e0242476.

Le Vine, S., Adamou, O., and Polak, J. (2014). "Predicting new forms of activity/mobility patterns enabled by shared-mobility services through a needs-based stated-response method: Case study of grocery shopping." *Transport Policy*, 32, 60-68.

Murtagh F., and Contreras, P. (2012). "Algorithms for hierarchical clustering: an overview." *WIREs Data Min. Knowl. Discov. 2,* 86–97.

Ongel A., Loewer E., Roemer F., Sethuraman G., Chang F., and Lienkamp, M. (2019). "Economic Assessment of Autonomous Electric Microtransit Vehicles." *Sustainability 11,* 648.

Pachal P. (2018). "Express Pool: cheaper rides, as long as you don't mind walking." *Mashable*. Accessed on: March 20, 2021. https://mashable.com/2018/02/21/uber-express-pool/

Pew Research Center. (2020). "Most Americans Say Coronavirus Outbreak Has Impacted Their Lives." Accessed on: August 15th, 2021. https://www.pewsocialtrends.org/2020/03/30/most-americans-say-coronavirus-outbreak-has-impacted-their-lives/

Schmitt, A. (2018). "The story of "micro transit" is a consistent, dismal failure." *Streetblog*.

Schaller, B. (2018). "Second chances: Regulation and deregulation of taxi and for-hire ride services." *TR News*, (315).

Statista. Monthly number of Uber's active users worldwide from 2016 to 2019. Retrieved from https://www.statista.com/statistics/833743/us-users-ride-sharing-services/

UTA On Demand, UTA. (2021). Accessed on: May 8, 2021 https://www.rideuta.com/Services/UTA-On-Demand

Volinski, J.. (2019). "Microtransit or General Public Demand–Response Transit Services: State of the Practice." *Transportation Research Board, 2019.*

WMATA. Metro and Covid-19: Steps we've taken. (2020). Accessed on: August 18, 2021. https://www.wmata.com/service/status/details/COVID-19.cfm

Westervelt M., Huang E., Schank J., Borgman N., Fuhrer T., Peppard C., and Narula-Woods, R. (2018). "UpRouted: Exploring Microtransit in the United States." *Eno Center for Transportation.*

Wilbur M., Ayman A., Ouyang A., Poon V., Kabir R., Vadali A., ... and Dubey, A.. (2020). "Impact of COVID-19 on public transit accessibility and ridership." arXiv preprint arXiv:2008.02413.

Xie, Y., Danaf, M., Azevedo, C.L., Akkinepally, A.P., Atasoy, B., Jeong, K., Seshadri, R., and Ben-Akiva, M. (2019). "Behavioral modeling of on-demand mobility services: general framework and application to sustainable travel incentives." *Transportation*, pp.1-23.

Xu Y., Chen D., Zhang X., Tu W., Chen Y., Shen Y., and Ratti, C. (2019). "Unravel the landscape and pulses of cycling activities from a dockless bike-sharing system." *Comput. Environ. Urban Syst. 75.* 184–203.

Yi, Z., Liu, X. C., Wei, R., Chen, X., and Dai, J. (2021). "Electric vehicle charging demand forecasting using deep learning model." *Journal of Intelligent Transportation Systems*, 1-14.

Yu, H., and Peng, Z.R. (2019). "Exploring the spatial variation of ridesourcing demand and its relationship to built environment and socioeconomic factors with the geographically weighted Poisson regression." *Journal of Transport Geography*, 75, pp.147-163.